Acta Geologica Polonica, Vol. 73 (2023), No. 4, pp. 801–832
DOI: 10.24425/agp.2023.148023

Detrital heavy minerals as guides to provenance of Albian arenites of southern extra-Carpathian Poland

JAKUB KOTOWSKI*, DANUTA OLSZEWSKA-NEJBERT and KRZYSZTOF NEJBERT

University of Warsaw, Faculty of Geology, Żwirki i Wigury 93, 02-089 Warszawa, Poland;
e-mails: j.kotowski@uw.edu.pl; dolszews@uw.edu.pl; knejbert@uw.edu.pl
** Corresponding author*

ABSTRACT:

Kotowski, J., Olszewska-Nejbert, D. and Nejbert, K. 2023. Detrital heavy minerals as guides to provenance of Albian arenites of southern extra-Carpathian Poland. *Acta Geologica Polonica*, **73** (4), 801–832. Warszawa.

The potential of heavy minerals as a provenance tracer in Albian arenites of extra-Carpathian Poland was assessed. Studies in this area have focused on various methods based on heavy mineral chemistry that provide an effective tool for reconstructing the provenance of quartz-rich sediments. The previously suggested division of the study area into two domains with different source areas: the western domain – the Miechów area, and the eastern domain – the Lublin area, was based on geochronological (monazite and muscovite dating) and rutile mineral chemical studies. The mineral chemistry of newly examined heavy minerals supports the previously suggested division. The mineral chemistry of detrital tourmaline suggests medium-grade metamorphic rocks as the main source in both domains. Detrital garnet in the western domain shows affiliation to the Góry Sowie Massif, while garnet in the eastern domain was most probably sourced from southern/central Norway. The western domain was most probably fed from rocks of the Bohemian Massif. The main source area for the eastern domain was most probably located in the Baltic Shield. The distinct division of the study area into two domains was caused by the palaeogeography of the region in the Albian and the action of longshore currents in south-eastward and eastward directions.

Key words: Detrital material; Mineral chemistry; Provenance; Stability of heavy minerals; Sand and sandstone; Lower Cretaceous.

INTRODUCTION

The clastic Albian sediments have a special place on the geological map of Poland. Clastic rocks of Middle and Late Albian age (c. 110.0–100.5 Ma) mark the beginning of a thick series of rocks from the Late Cretaceous transgression (Leszczyński 2010, 2012). During the Early Cretaceous, the sedimentation was generally restricted to the axial part of the Mid-Polish Trough (Leszczyński 1997). In the Albian, the sea encroached into the territory of Poland from the northwest (Marcinowski and Radwański 1983) and possibly also from the southeast (Krassowska 1976). During the Albian, most of the area of present-day extra-Carpathian Poland flooded by a shallow sea was called the Polish Basin (Stephenson *et al.* 2003; Dadlez *et al.* 2005). In the first stages of the transgression, relatively thick layers of sand were deposited on land areas built mainly of Upper Jurassic carbonates. Most of the Albian sands/sandstones are devoid of index fossils, but ammonites were found in two places in the Miechów area, which indicated a Late Albian age (Hakenberg *et al.* 1973; Marcinowski and Wiedman 1990). With continuation of the transgression, the Albian sediments were covered by various Cenomanian marly carbonate or carbonate sediments, very well documented by fossils (Marcinowski 1970, 1974; Hakenberg *et al.* 1973; Marcinowski and

Radwański 1983, 1989). The source areas of detrital material in Albian sedimentary rocks in Poland have been of interest to geologists for nearly a century (Samsonowicz 1925; Marcinowski 1974; Hakenberg 1986). The origin of such a large amount of detrital material has not yet been fully established. Initially, the focus was mainly on observing sedimentary structures and stratigraphy, and deducing the direction of material transport (Marcinowski 1974; Cieśliński 1976; Hakenberg 1986). The suggested directions of transport from the south, i.e., the Bohemian Massif into the Miechów area (Hakenberg 1986) and from the Ukrainian Shield into the Lublin area (Hakenberg and Świdrowska 2001) were based only on the principle of proximity to crystalline rocks in relation to the study areas. However, analysing only these aspects seems insufficient and can lead to false conclusions about the origin of the clastic material. In many cases of transgressive sediments, visible cross-bedding may have come from the washing away of loose sediment by coastal currents the direction of which is closely related to the shape of the local coastline (Rudowski 1962; Kuhrts *et al.* 2004; Liu *et al.* 2017). Another approach to determining the source of clastic material (especially in ancient deposits) is to study the chemical composition of heavy minerals, i.e., accessory minerals with a density higher than 2.85 g/cm^3 (Mange and Wright 2007). In the case of relatively young sedimentary rocks and those that have not undergone significant diagenesis and chemical weathering, the quantity and variety of heavy minerals could be used as a proxy in provenance studies (e.g., Morton 1991; Garzanti and Andò 2007a, b; Mange and Morton 2007; Garzanti *et al.* 2010, 2019). Varietal studies, considering different groups of detrital minerals can provide a lot of information regarding the petrography of source rocks (Mange and Wright 2007) and also about the climate and diagenetic processes of heavy minerals (HM; Weibel and Friis 2007; Andò *et al.* 2012). Multiple recycling that is not properly considered in many provenance studies (Garzanti 2017) may also effectively control the amount of HMs. Thanks to the rapidly developing analytical techniques (e.g., sensitive high-resolution ion microprobe – SHRIMP, Multi Collector Laser Ablation Inductively Coupled Plasma Mass Spectrometry – MC-LA ICP MS, electron microprobe – EPMA), it has become possible to study precisely the variability of chemical composition and isotopic ratios in many heavy minerals (e.g., Garzanti *et al.* 2010; Akdoğan *et al.* 2017; Flowerdew *et al.* 2020; Szopa *et al.* 2020; Kowal-Linka *et al.* 2022). This, in turn, made it possible to use subtle changes in their isotopic ratios and chemical composition to determine the age, crystallisation conditions and lithology of the initial source rock. By using several different heavy minerals co-occurring in the Albian sediments, it has become possible to get a clearer picture of the initial source area(s) and rocks that build them (Kotowski *et al.* 2020, 2021, 2023).

The aims of this paper are: (1) to comment and supplement information about the minerals described in previous studies (Kotowski *et al.* 2020, 2021, 2023); (2) to test the compositions of other non-opaque (transparent) and selected opaque heavy minerals with provenance; (3) to report the influence of weathering processes on heavy minerals; and (4) to point out the lithological and palaeogeographic source of the sandy detrital material.

GEOLOGICAL SETTING

The study area is located in southern Poland, north of the Carpathian nappes (Text-fig. 1). The thickness of the Albian sediments in Poland is not uniform (Text-fig. 2). The highest values can be found in central Poland where the highest subsidence rates are assumed (Jaskowiak-Schoeneichowa and Krassowska 1988; Leszczyński 1997; Świdrowska *et al.* 2008). In the Lublin area in eastern Poland numerous, although limited in size, areas with a reduced thickness or absence of Albian sediments were recorded by Jaskowiak-Schoeneichowa and Krassowska (1988). The areas without Albian sediments are located mainly in the southern and eastern parts of Poland, and the regions of Gdańsk and Kętrzyn in northern Poland (Text-fig. 2).

In the area of the Miechów Segment, Albian outcrops are limited to NW-SE-trending narrow belts on the trough margins (Text-fig. 1C), and a few outcrops in the area of the Chełmo Mount (part of the Radomsko Folds that terminate the Miechów Segment from the north). In the western part of the trough at the boundary with the Kraków-Częstochowa Upland, the Albian is represented by very similar lithofacies, i.e., white and grey quartz sands or loosely cemented sandstones with glauconite admixtures, and with sparse silicification in the form of discontinuous horizontal beds.

East of the Holy Cross Mountains (HCM) the Albian rocks are covered by a thick succession of Upper Cretaceous rocks and can be accessed only in boreholes, mines, or scarce outcrops (e.g., Kopiec in the vicinity of Annopol). The Albian arenites in most of the Lublin area occur in a similar position as in the Miechów Segment, i.e., on Upper

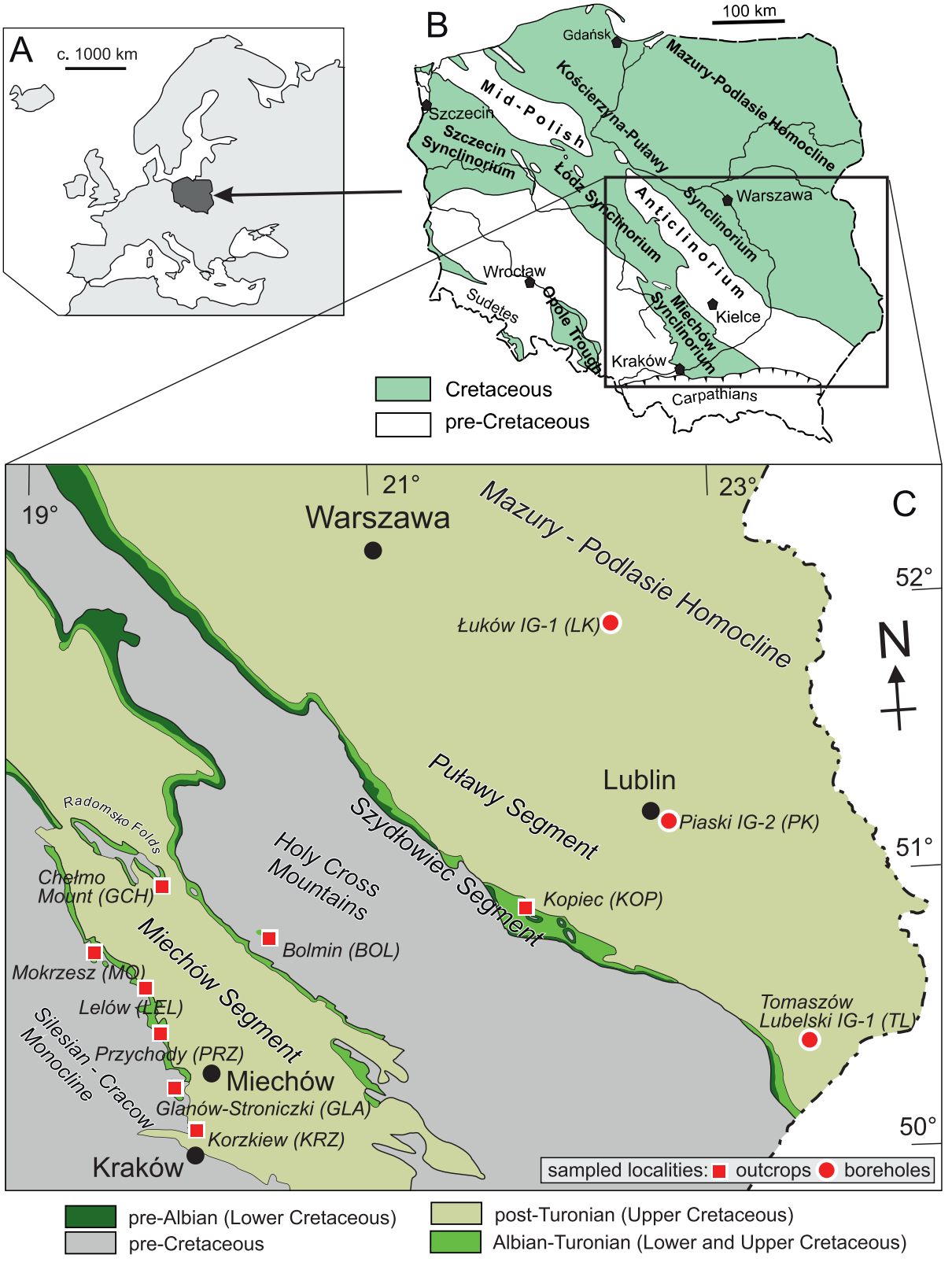

Text-fig. 1. Simplified geological maps showing the extent of Cretaceous deposits in Poland, without the Cenozoic cover. A – location of Poland in Europe; B – tectonic sketch map of Poland (after Żelaźniewicz *et al.* 2011) and location of the study area; C – simplified geological map of Miechów and Lublin areas (modified after Dadlez *et al.* 2000) with sampled locations.

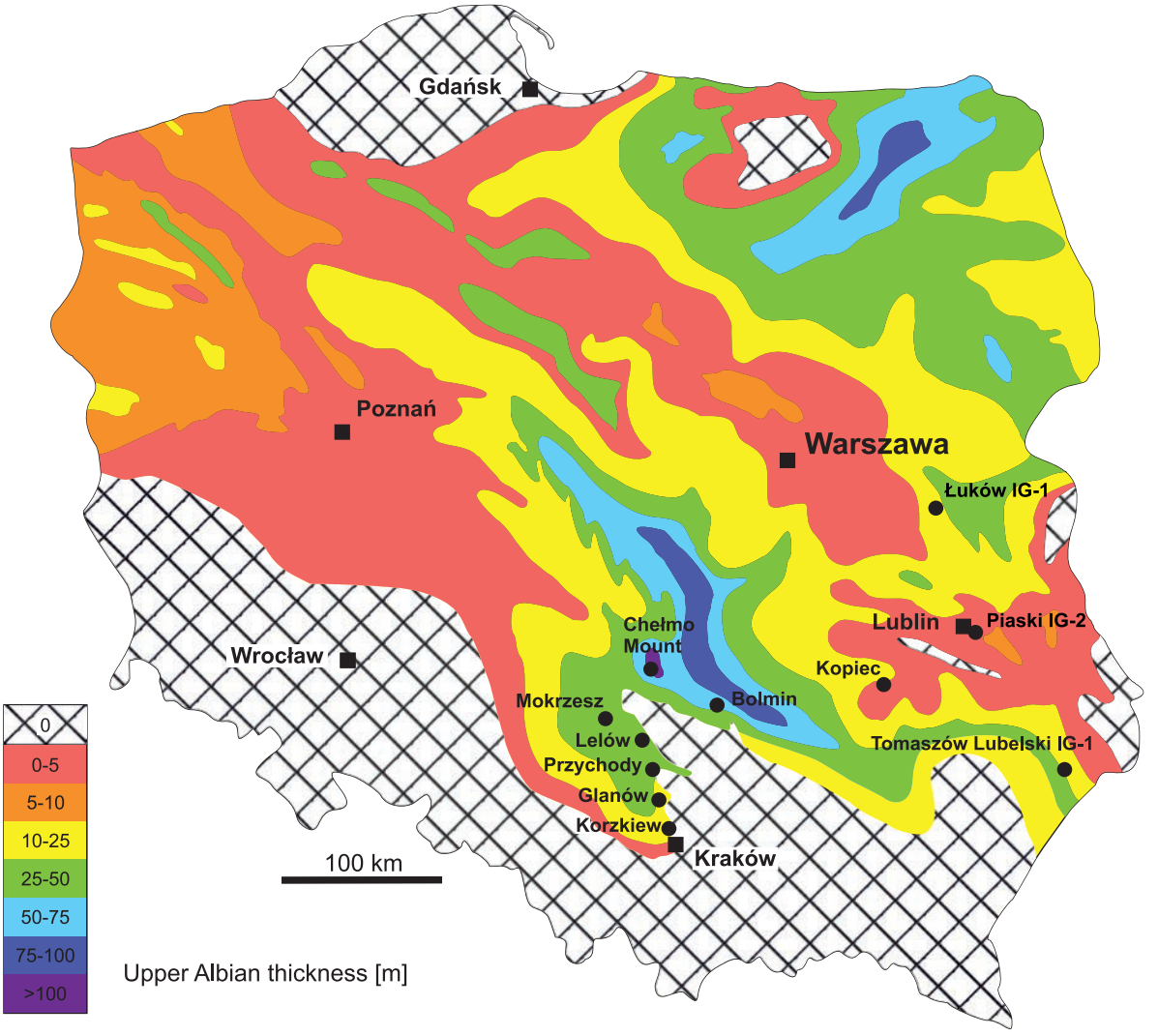

Text-fig. 2. Thickness of the Upper Albian in Poland, modified after Jaskowiak-Schoeneichowa and Krassowska (1988).

Jurassic carbonates; only in easternmost Poland (east of Zamość), the Albian and Cenomanian rocks lie on Carboniferous mudstones, siltstones, and sandstones. The local thickness distribution was largely influenced by the pre-Albian topography. In most of Poland, the transgression entered an area of already varied topography (Hakenberg 1978). The transgression propagated mainly from the Bornholm region southwards onto the Polish Lowlands (Marcinowski and Radwański 1983). However, a minor connection with the Tethys in the S-SE of Poland also must have existed, as shown by the faunal influence from the Tethyan Sea (Marcinowski and Radwański 1983; Marcinowski and Wiedmann 1985; Machalski and Kennedy 2013). The transgression developed along the Mid-Polish Trough, an area of increased subsidence present already since the late Permian (Dadlez 2003), and then the epicontinental sea propagated perpendicularly to its axis (Krassowska 1976). Albian deposits, as well as the Upper Cretaceous strata, were eroded from the HCM during the Alpine orogeny after the inversion of the Mid-Polish Trough when Jurassic, Triassic, and Palaeozoic rocks were exposed (Kutek and Głazek 1972).

MATERIAL AND METHODS

Eleven locations were sampled: seven samples from the Miechów area and four from the Lublin area (Text-figs 1 and 3). Five samples were taken from outcrops in the western part of the Miechów area at

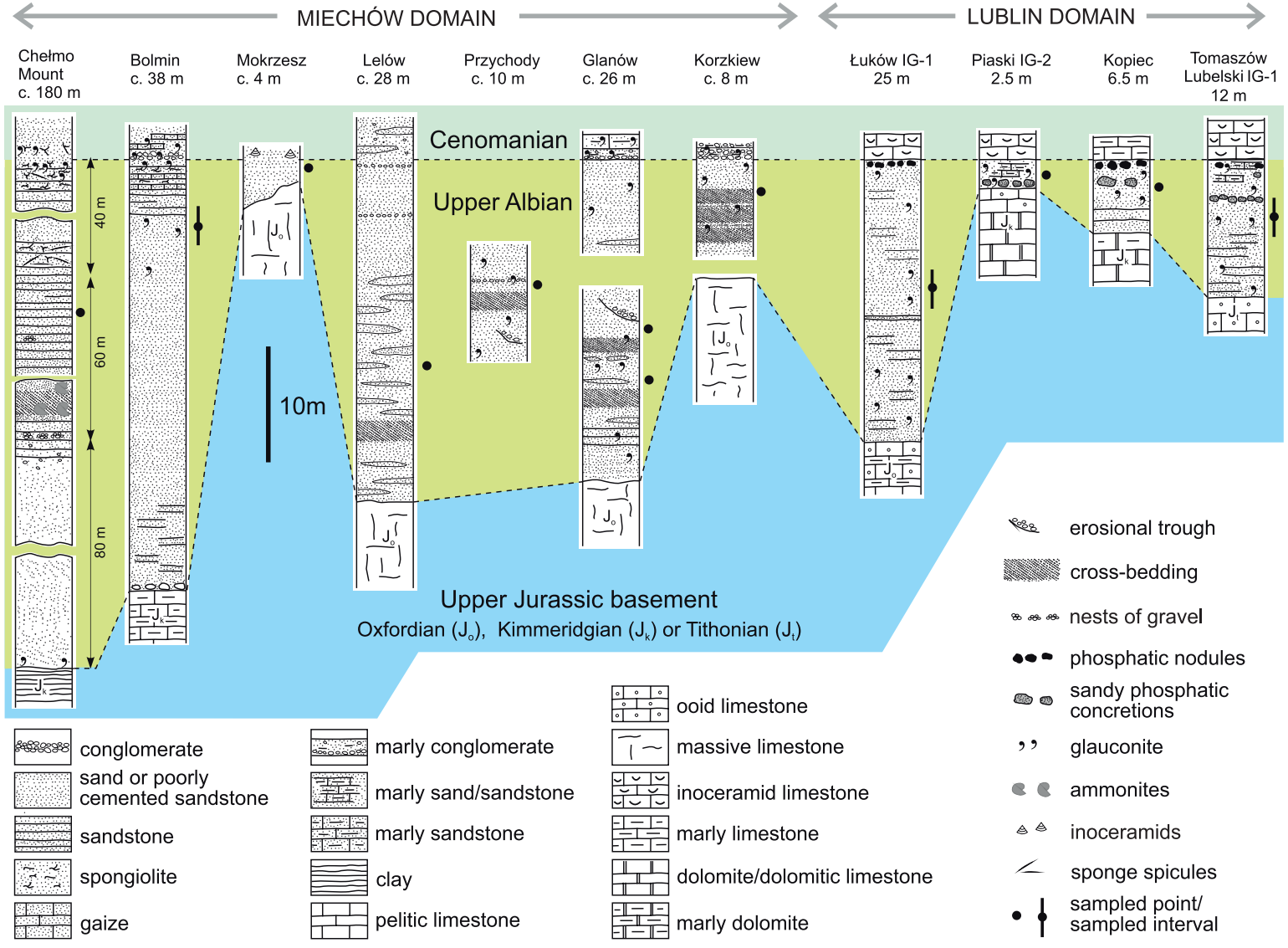

Text-fig. 3. Simplified correlation of Albian deposits from studied sections in southern extra-Carpathian Poland with indicated sampled points or intervals. Geological data for outcrops from Hakenberg *et al.* (1973); Marcinowski (1974); Chlebowski *et al.* (1978); Małecki (1980) and own observations; for boreholes from Lendzion and Wierzbowski (1966), Żelichowski and Rek (1966), and Gurba (1984).

Korzkiew (KRZ), Glanów-Stroniczki (GLA), Lelów (LEL), Przychody (PRZ), and Mokrzesz (MO). One sample from the Bolmin (BOL) outcrop was sampled from the eastern part of the Miechów area. The location of the sample collected from the Chełmo Mount (GCH) is on the northern border of the Miechów area, which separates it from the Mogilno-Łódź Segment, located further to the north. Almost all samples in the Miechów segment are represented by loose quartz sands (Text-fig. 4A, B, I, J). Only in the Chełmo Mount the Albian clastic rocks are represented as cemented grey sandstone/quartz arenites (Text-fig. 4C, K). One sample from the Kopiec outcrop (KOP; Text-fig. 4N) and three samples from boreholes (Tomaszów Lubelski IG-1, Piaski IG-2, and Łuków IG-1) were taken from the Lublin area (Text-fig. 4D, E–H, L, M).

On the eastern side of the present-day HCM, access to Albian rocks is available mainly in boreholes under a thick cover of Upper Cretaceous carbonate deposits. The only sampled outcrop, which is located close to the village of Kopiec near Annopol on the River Vistula, is situated in the north limb of the Annopol Anticline. The locations of the sampled material from boreholes were selected based on the availability of core material and the best possible coverage of the studied area. Tomaszów Lubelski IG-1 (TL) is the southeasternmost borehole with Albian sediments in the study area and was sampled at a depth of 1006.7–1013.0 m b.g.l. Further north, samples were taken from the Piaski IG-2 (PK) borehole near Lublin (sampled interval depth of 725.4–727.4 m b.g.l.) and Łuków IG-1 (LK) borehole (sampled interval depth of 510.1–524.6 m b.g.l.), being the northeasternmost point in the study area (Text-fig. 1).

In heavy mineral separation, two methods were used. The first separation method was used to obtain a large number of heavy minerals for chemical analysis. For this method, a 1 kg sample from each outcrop was taken; however, due to the limited amount of borehole material c. 0.5 kg of core sample was used for further analyses. The lithified sandstone samples from the Chełmo Mount were initially crushed with a Testchem LKS-60 jaw crusher. All samples were then sieved, and 63 to 250 μm fraction grains were designated for further mineral chemistry analysis. Samples were separated into magnetic fractions (0.3 A, 0.5 A, 1.2 A) with the Franz LB-1 Magnetic Barrier Laboratory Separator and then separated into heavy mineral fractions using LST Fastfloat heteropolytungstate with a density of 2.9 g/cm^3. The obtained heavy mineral samples were embedded in epoxy resin and polished for SEM and EPMA analysis. In the second method of separation, 100 g of rough samples (neither sieved nor separated magnetically) from each location were separated using only LST density separation for further description (e.g., grain size) and quantitative analysis. A minimum of 630 HM grains per sample (min. 250 transparent HMs) mounted on conductive carbon tape were randomly counted using the SEM-EDS method. Some distinctive heavy minerals, such as monazite, rutile, and tourmaline, were handpicked and mounted separately in epoxy resin. Grain surface morphology and initial phase identification were carried out at the Laboratory of Electron Microscopy, Microanalysis, and X-ray Diffraction, Faculty of Geology, University of Warsaw, on a ZEISS SIGMA VP field emission electron microscope (FE-SEM) equipped with two X-ray energy-dispersive Bruker XFlash 6|10 spectrometers (SEM-EDS). The high-resolution digital microscope KEYENCE VHX-7000 was used to observe and make photographic documentation of rough arenites. Photomicrography of selected heavy minerals was done on a Delta Optical POL-1000TRF petrographic optical microscope with and without immersion oil. The Cargille immersion Oil Type A, with 1.515 refractive index at 23ºC using sodium D Line (589.3 nm) were used. The viscosity of the oil at 23ºC is close to 150 cSt. Opaque minerals were identified and photographed using a Nikon E600 optical microscope, working in reflected polarised light. Chemical analyses of tourmaline (413 analyses), garnet (152), staurolite (182), zircon (225), Cr- (325) and Zn-spinels (74 analyses) were conducted on a CAMECA SX-100 electron microprobe (EPMA),

Text-fig. 4. Photographic documentation of selected outcrops, core materials and rough sands from the study area, Albian, uppermost Lower Cretaceous. A – abandoned sand-pit in Glanów-Stroniczki; B – abandoned sand-pit in Lelów, C – abandoned sandstone quarry in Chełmo Mount; D – fragment of core, Tomaszów Lubelski IG-1, depth 1006.7–1013.0 m b.g.l.; E – fragment of core, poorly cemented fine-grained sand, Piaski IG-2, depth 725.4–727.4 m b.g.l.; F-H – fragments of core, Łuków IG-1, depth 510.1–524.6 m b.g.l.; view of the crushed material housed in a wooden box, sand and sandstone poorly cemented by clay minerals (F); sand and poorly cemented sandstone with an admixture of glauconite (G, H); I–N – photomicrograph of rough sands and sandstone; I – loose fine-grained quartz sands with admixture of glauconite, Glanów-Stroniczki; J – loose medium-grained quartz sands with admixture of glauconite, Lelów; K – fine-grained quartz sandstone cemented by silica and clay minerals, Chełmo Mount; L – loose fine-grained quartz sands with admixture of glauconite, Tomaszów Lubelski IG-1; M – loose fine-grained quartz sands with admixture of glauconite, Łuków IG-1; N – loose coarse-grained quartz sands with admixture of phosphorites and glauconite, Kopiec. Fsp – feldspar; Grt – garnet; Glt – glauconite; Ms – muscovite; Qz –quartz; ph – phosphorite. →


A
2m
B
2m
C
D
11 12 13 14
F
5cm
I
Glt
Qz
Fsp
Ms
250 µm
G
2 3 5m 4 5 6 7
J
Glt
Qz
Fsp
250 µm
E
2cm
H
2cm
K
Qz
250 µm
L
Qz
Glt
250 µm
M
Glt
Ms
Qz
250 µm
N
Glt
Qz
Grt
ph
250 µm

while monazite and rutile chemistry analyses were performed on a CAMECA SX-FIVE field emission electron microprobe, both at the Laboratory of Electron Microscopy, Microanalysis and X-ray Diffraction at the Faculty of Geology, University of Warsaw. A complete set of chemical analyses is provided in Supplementary Online Material 1. The detailed conditions for EPMA chemical analyses are in the Supplementary Online Material 2. Transparent, columnar minerals were handpicked from the non-magnetic heavy mineral fraction for identification by X-ray diffraction. The phase composition study was carried out using an XPERT PRO diffractometer at the Laboratory of Electron Microscopy, Microanalysis and X-ray Diffraction at the Faculty of Geology, University of Warsaw, with the following parameters: Co Kα wavelength, generator settings of 35 mA, and 40 kV current. X-ray patterns were collected over a range of 6º to 78º 2Θ with a step size of 0.026º 2Θ. Phase analyses of K-feldspars and Fe-Ti oxides were done using a Renishaw inVia Qontor Raman spectrometer with 532 nm laser excitation, 50 mW laser power, 1800 lines/mm grating and a Peltier-cooled CCD detector. Single spot analyses were made using a 100x objective.

RESULTS

The studied samples (LK, PK, GLA, GCH, TL) are fine-grained and medium-grained (BOL, PRZ, KRZ, LEL, MO) sands; only the sample from Kopiec (KOP) can be classified as coarse sand (Text-fig. 5). The coarse-grained sand in Kopiec is most likely a result of numerous coarse phosphorite grains in the sample; the detrital grains (mainly quartz) being medium-grained in size. Studied samples are well- to moderately-sorted (Text-fig. 5), and only the sample from Bolmin (BOL) is poorly sorted sand. Most of the detrital grains in the studied samples are quartz (over 90%), Na-plagioclase (albite), and K-feldspar, i.e., orthoclase and subordinate microcline (both up to 8%). Apart from heavy minerals, low amounts of muscovite, glauconite, large feldspar grains above 1 mm (microcline, orthoclase, albite) and lithic fragments can be found. In most cases, lithic fragments are coarse-grained (>0.5 mm in diameter) and represent older fine-grained clastic rocks (i.e., claystone, mudstone, or fine-grained sandstone/quartzite), cherts, phosphorites (mostly in samples from the Lublin area), granites, gneisses, quartz schists and silicified wood (in sample GLA; Text-fig. 6).

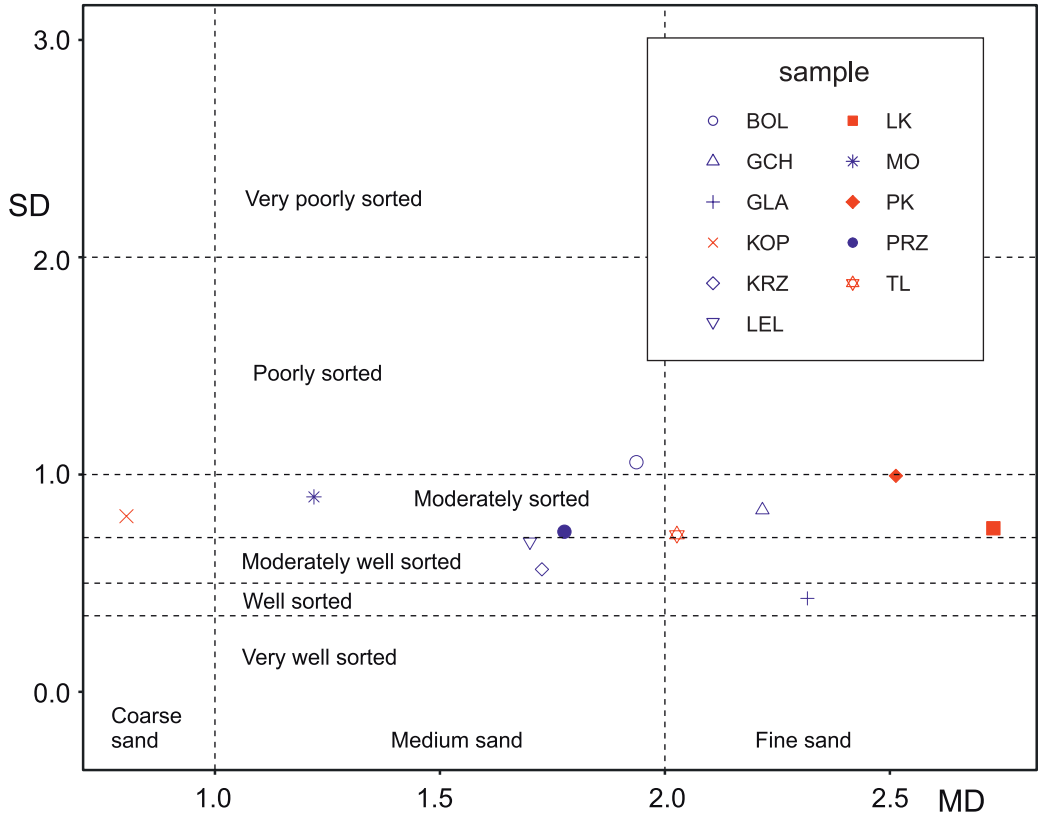

Text-fig. 5. Results of granulometric study presented on a binary plot of mean diameter (Phi) – MD against standard deviation – SD based on Blott and Pye (2001).

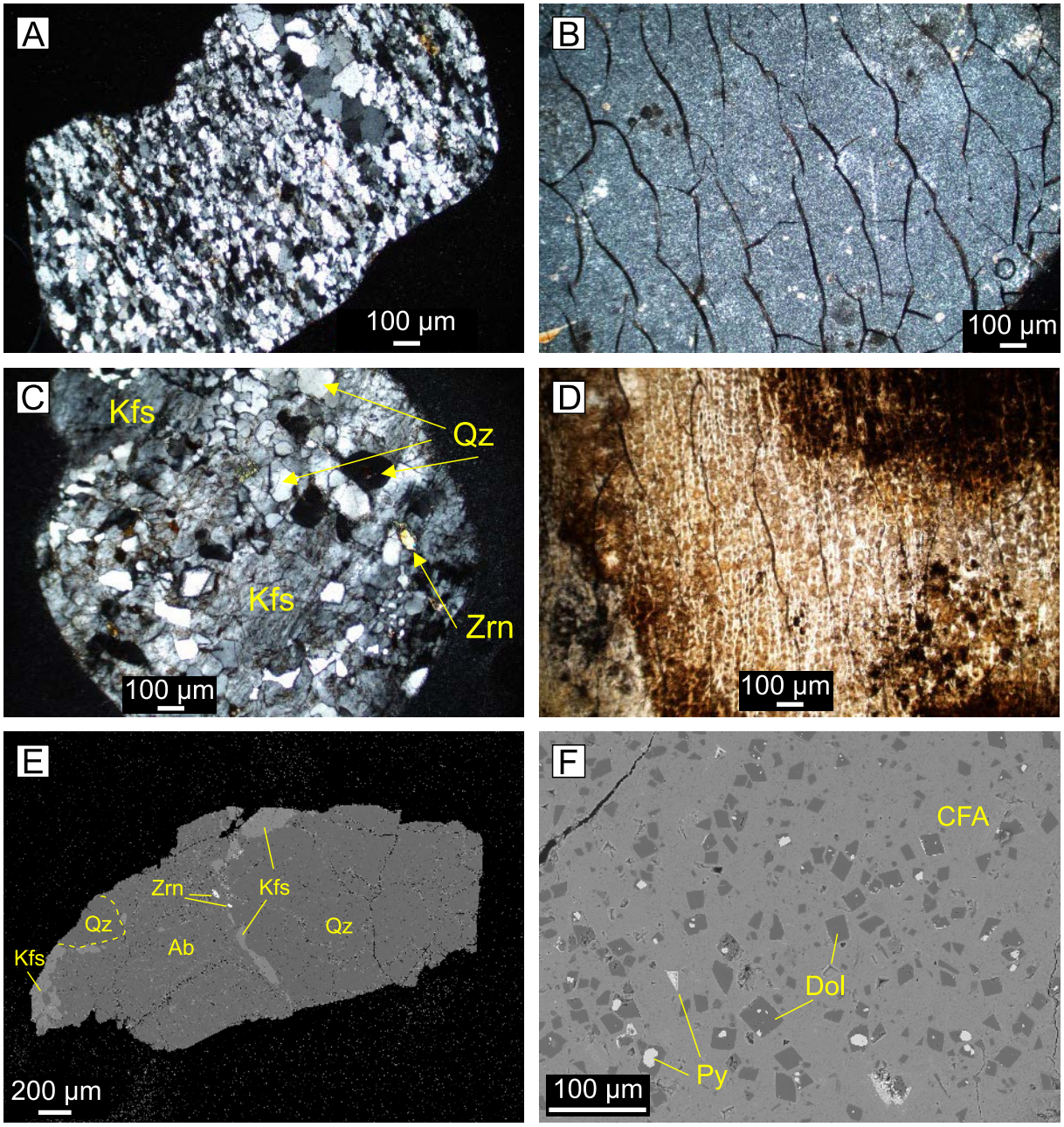

Text-fig. 6. Thin-section photomicrographs of lithic fragments in Albian arenites. A – fragment of quartz schist from Lelów, cross-polarized light; B – chert fragment from Łuków IG-1 borehole, cross-polarized light; C – igneous rock fragment (most probably granite) from Glanów-Stroniczki, cross-polarized light; D – fragment of silicified wood from Glanów-Stroniczki, transmitted light; E – SEM-BSE image of granite, fragment from Łuków IG-1 borehole; F – SEM-BSE image of phosphorite intraclast from Piaski IG-2 borehole. Ab – albite, CFA – carbonate fluorapatite, Dol – dolomite, Kfs – K-feldspar, Py – pyrite, Qz – quartz, Zrn – zircon.

The heavy mineral assemblage of transparent (non-opaque) minerals dominates over opaque minerals (Text-fig. 7). The most frequent minerals among the transparent group are zircon, rutile, tourmaline, monazite, garnet, staurolite, and kyanite (Text-figs 7 and 8). The opaque group consists of ilmenite, leucoxene – pseudomorph after ilmenite and Ti-magnetite, as well as magnetite and Cr-spinel. The results of Raman spectroscopy indicate that anatase is the main component in leucoxene pseudomorphs.

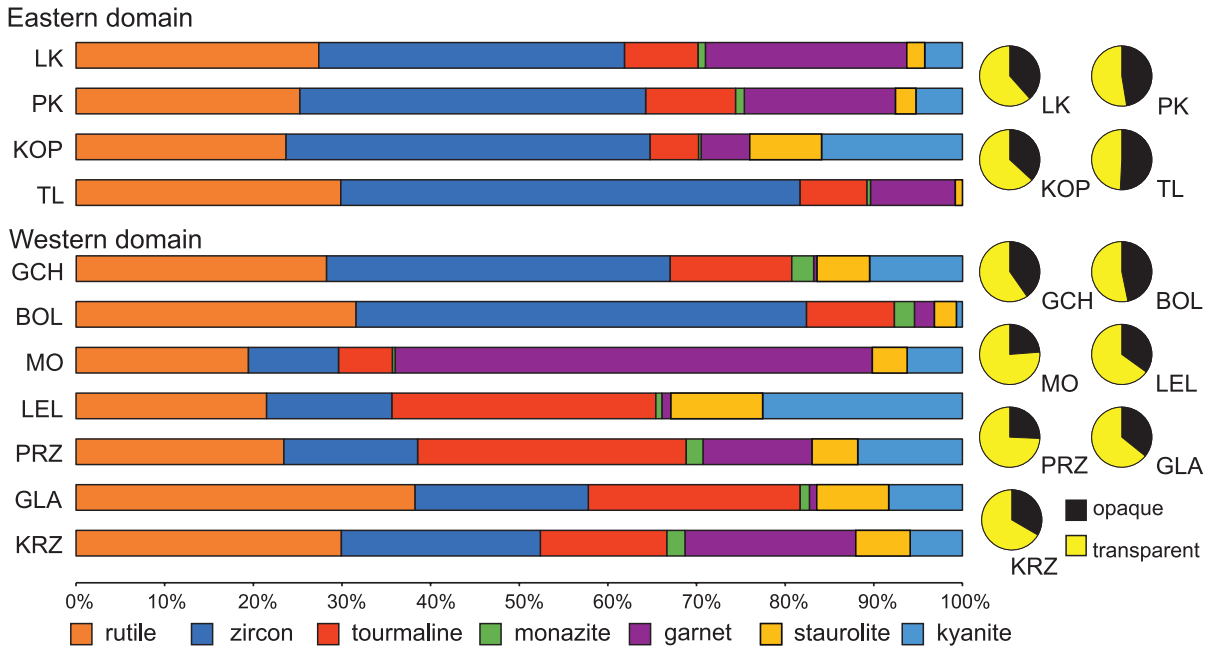

ZTR index [%]

Western domain							Eastern domain			
GCH	BOL	MO	LEL	PRZ	GLA	KRZ	LK	PK	KOP	TL
78.6	88.9	34.9	64.8	68.3	79.9	65.6	68.9	72.8	68.8	88.9

Text-fig. 7. Composition of transparent heavy minerals, the ZTR (Zircon Tourmaline Rutile) index, and pie charts of opaque and non-opaque (i.e., transparent) minerals from the Albian arenites of southern Poland.

The other sporadically occurring heavy minerals, both opaque and transparent, are titanite, cassiterite, gahnite, and xenotime. The full dataset of EPMA analyses is available in Supplementary Material 1.

Zircon

Zircon constitutes 10% to 52% (on average 31%) of all transparent heavy minerals in the studied material (Text-fig. 7). The most numerous grains are colourless, yellowish, and light orange. Their size is quite variable, from 40 μm to c. 200 μm, and the grains are euhedral, subangular, and subrounded to well-rounded in shape (Text-fig. 8B). According to Andò *et al.* (2012), the degree of corrosion based on visual classification of surface textures can be described as an unweathered or initial stage. Most zircon grains do not show a significant degree of weathering even in high magnifications. The results of chemical analyses obtained from the EPMA study are nearly uniform across the samples. Only slight variations in the concentrations of Hf can be noticed, ranging from 0.82 to 1.83 wt%.

Text-fig. 8. Heavy minerals from the Albian sands of southern Poland, arranged in order of persistence (adopted from Pettijohn 1941); biotite → and white mica are not included in the mentioned order; all grains from Glanów-Stroniczki, except garnet F_1 which is from Mokrzesz. A_1–A_6 – rutile, images A_2–A_5 in immersion oil; A_1, A_2 – angular grains, A_3, A_4 – subangular grains, A_5, A_6 – subrounded grains; B_1–B_5 – zircon; B_1, B_2 – euhedral grains, B_3 – subrounded grain, B_4 – subrounded euhedral grain, B_5 – well-rounded grain; C_1–C_8 – tourmaline, all images in oil; C_1 – angular grain, C_2 – subangular grain, C_3 – euhedral subangular grain, C_4, C_5 – euhedral subangular/subrounded grains, C_6, C_7 – subrounded grains, note the blue core and brown rounded envelope on C_6, common in pegmatite (e.g., Pieczka *et al.* 2013), C_8 – rounded grain; D_1–D_5 – rare spinel grains of gahnite, D_3, D_4 in immersion oil; D_1 – angular grain, D_2, D_3 – subrounded grains, D_4 – rounded grain, D_5 – well-rounded grain; E_1–E_6 – monazite, E_1 in immersion oil; E_1 – subangular grain, E_2–E_4 – subrounded grains, E_5 – rounded grain, E_6 – well-rounded grain; F_1–F_6 – garnet, F_1 in reflected light, F_2–F_6 in immersion oil; F_1, F_2 – angular grain, F_2–F_5 – subrounded grains, F_6 – well-rounded grain; G_1–G_4 – staurolite, all images in immersion oil; G_1–G_3 – subangular grains, G_4 – subrounded grain; H_1–H_4 – kyanite; H_1–H_3 – angular grains, H_4 – subangular grain; I_1, I_2 – titanite, all images in immersion oil; I_1 – angular grain, I_2 – subangular grain; J_1, J_2 – biotite; J_1 – subangular grain partly preserved as pseudohexagonal crystal, J_2 – subrounded grain; K_1, K_2 – white mica, K_2 in immersion oil; K_1 – subrounded grain, K_2 – subangular grain.

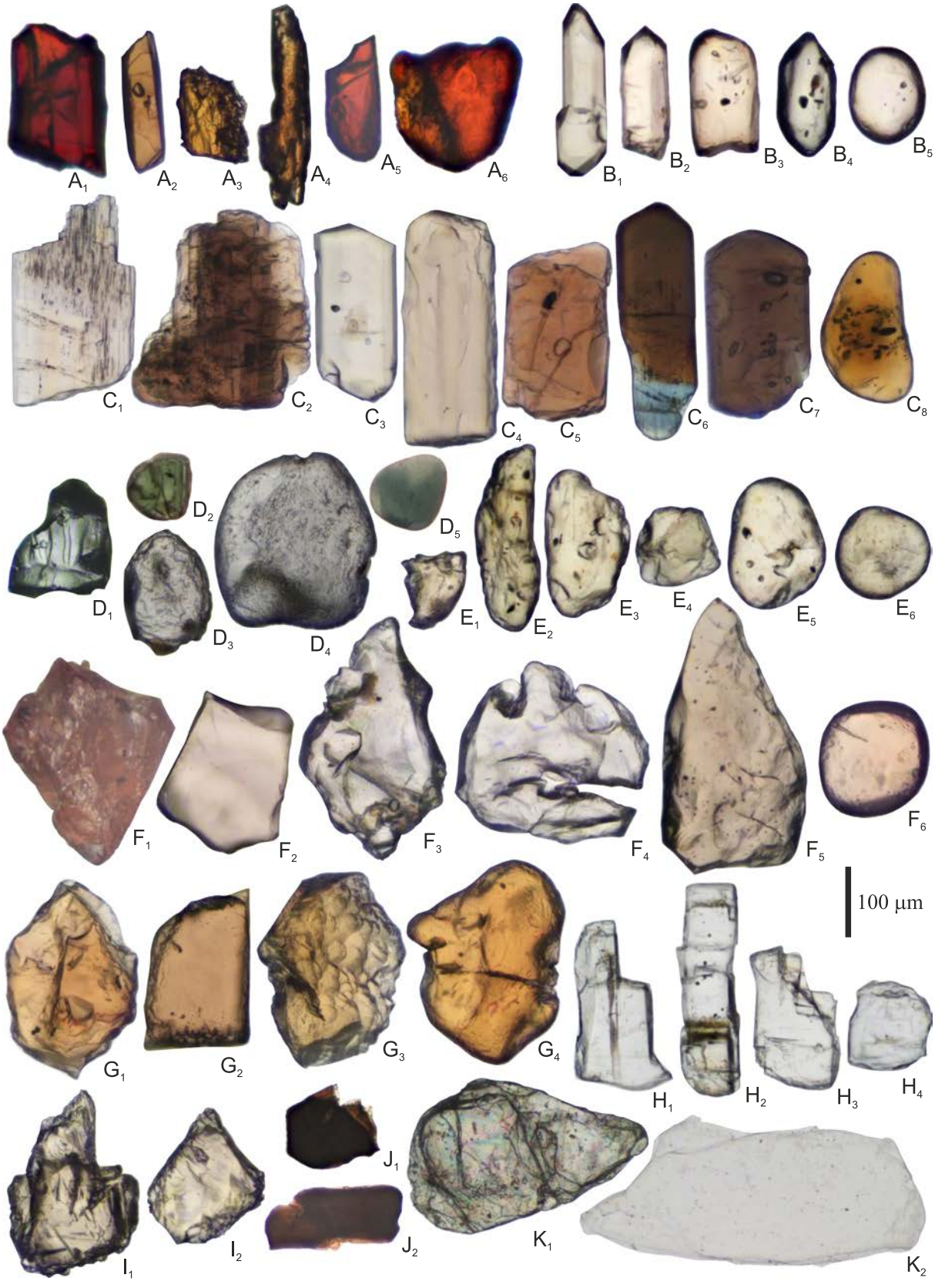
A1
A2
A3
A4
A5
A6
B1
B2
B3
B4
B5
C1
C2
C3
C4
C5
C6
C7
C8
D1
D2
D3
D4
D5
E1
E2
E3
E4
E5
E6
F1
F2
F3
F4
F5
F6
100 µm
G1
G2
G3
G4
H1
H2
H3
H4
I1
I2
J1
J2
K1
K2

Tourmaline

Tourmaline from the Lublin area constitutes up to 10.2% (on average 7.9%) of all transparent heavy minerals. The most numerous tourmaline grains are brown, yellowish, light orange, and colourless. In core samples, especially those in the northeastern part of the study area (samples LK and PK), tourmalines are mostly euhedral and subrounded ranging predominantly from about 20 μm to 150 μm. Larger grains are rare and generally well rounded. A degree of corrosion can be described as unweathered, in the initial and slight stage (Andò *et al.* 2012). Most tourmalines do not show a significant degree of weathering and alteration. The majority of tourmaline grains are dravite and schorl (Text-fig. 9) with only, minor amounts of uvite, foitite and Mg-foitite (respectively 1.5%, 0.3%, and 0.3% of all tourmaline grains). The percentage of tourmaline species does not differ significantly between studied localities. Some tourmalines express a distinct zonation regarding their chemical composition. However, there is no clear correlation between the chemical composition of a particular zone and sample location. The concentration of Ti is in the range of 0.01 to 0.26 apfu with an average of 0.08 apfu. Only trace amounts of Cr and V were detected in analysed tourmalines, on average 0.09 and 0.03 apfu respectively (Table 1). Concentrations of Mn and Zn are mostly below the detection limit.

Spinel

Most of the spinel group minerals found in studied samples are Cr-spinels (chromite and magnesiochromite) with only several grains being Zn-spinels (gahnite) and magnetite. Spinel grains are mostly below 150 μm in size with various degrees of abrasion, erosion, and roundness (Text-fig. 8D). Most grains are fairly well rounded with etch marks on their surface visible in SEM imaging. Gahnite grains are mostly light blue to greenish-blue in colour, while Cr-spinels are typically black, rounded, and partially cracked. Chromium spinels have a very wide range of chemical compositions. Concentrations of Cr_2O_3 range from 8 wt% to over 65 wt%. Abundances of the other main cations, such as Fe, Mg, and Al, are also quite variable (Table 2). A more significant difference can be seen in the TiO_2 content in the spinel structure. In samples from the Miechów area, the content of TiO_2 varies between 0.12 wt% and 0.21 wt%. Only spinels from samples GLA and BOL have higher levels (0.27 wt% and 0.31 wt% of TiO_2, respectively). Spinels from LK and PK (northeasternmost samples) have TiO_2 contents averaging 0.46 wt%. The KOP sample (geographically close to the TL sample) has values similar to those from the Miechów area, averaging 0.2 wt% TiO_2. The X_{Cr} [i.e., $Cr/(Cr+Fe_{tot})$] is on average 0.64 and X_{Mg} [i.e., $Mg/(Mg+Fe_{tot})$] is 0.48 for all samples. The concentrations of Cu, Nb, Zr, Sc, Sn, Co, and Ni are mostly below the detection limit of the electron

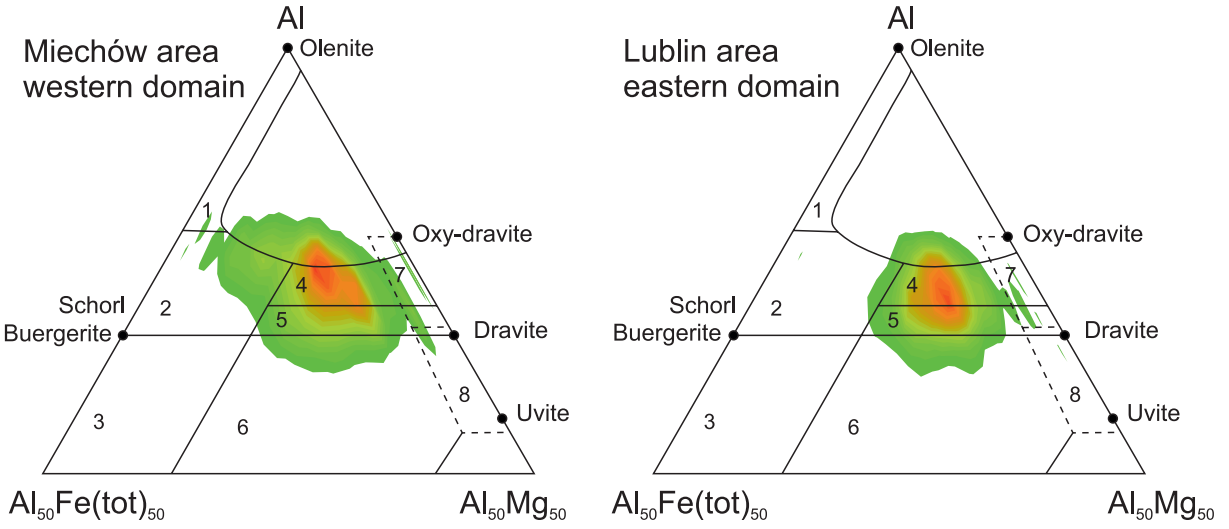

Text-fig. 9. Al-Fe-Mg ternary diagram of Henry and Guidotti (1985) for tourmalines from the Miechów and Lublin areas. (1) Li-rich granitoid pegmatites and aplites, (2) Li-poor granitoids and their associated pegmatites and aplites, (3) Fe^{3+}-rich quartz-tourmaline rocks (hydrothermally altered granites), (4) Metapelites and metapsammites coexisting with an Al-saturating phase, (5) Metapelites and metapsammites not coexisting with an Al-saturated phase, (6) Fe^{3+}-rich quartz-tourmaline rocks, calc-silicate rocks, and metapelites, (7) Low-Ca metaultramafites and Cr, V-rich metasediments, (8) Metacarbonates and metapyroxenites. Note the overlap of fields 4 and 5 with field 7.

Sample	KRZ-1 x6	GLA-1 x14	Mo-1 x25	Tom_Lub_11	Piaski_42	LKD_3a
	KRZ	GLA	MO	TL	PK	LK
Major constituents (wt%)						
SiO_2	34.32	37.13	36.66	35.81	35.99	35.60
TiO_2	0.70	0.43	0.82	1.24	0.75	0.29
B_2O_3*	10.08	10.77	10.65	10.47	10.56	10.60
Al_2O_3	30.01	32.94	32.05	31.49	33.68	31.93
V_2O_3	0.02	0.04	0.13	0.13	0.00	0.00
Cr_2O_3	0.00	0.00	0.01	0.00	0.00	0.00
FeO	16.07	4.88	5.13	8.09	6.83	5.41
MgO	1.91	7.81	7.75	5.99	5.34	8.98
MnO	0.03	0.09	0.05	0.00	0.00	0.12
CaO	0.76	0.59	0.48	0.74	0.92	1.76
ZnO	0.00	0.05	0.10	0.00	0.00	0.00
Na_2O	2.16	2.23	2.36	1.82	1.58	1.51
K_2O	0.09	0.02	0.01	0.00	0.07	0.08
F	0.45	0.02	0.06	0.00	0.16	0.19
H_2O*	3.26	3.71	3.65	3.61	3.57	3.57
O=F	0.19	0.01	0.02	0.00	0.07	0.08
Total	99.66	100.69	99.88	99.39	99.38	99.96
Calculated formulae (apfu)						
T-site						
Si^{4+}	5.920	5.991	5.982	5.946	5.923	5.835
Al^{3+}	0.080	0.009	0.018	0.054	0.077	0.165
Y-, Z-site						
Al^{3+}	6.021	6.256	6.145	6.108	6.456	6.002
Ti^{4+}	0.091	0.052	0.100	0.155	0.092	0.036
Cr^{3+}	0.000	0.000	0.001	0.000	0.000	0.000
V^{3+}	0.003	0.006	0.017	0.017	0.000	0.000
Fe^{2+}	2.318	0.659	0.701	1.124	0.940	0.741
Mn^{2+}	0.004	0.012	0.007	0.000	0.000	0.017
Mg^{2+}	0.491	1.878	1.885	1.482	1.310	2.193
Zn^{2+}	0.000	0.006	0.012	0.000	0.000	0.000
Subtotal	8.928	8.869	8.868	8.886	8.798	8.989
X-site						
Ca^{2+}	0.140	0.102	0.083	0.132	0.161	0.309
Na^{+}	0.721	0.697	0.747	0.585	0.503	0.480
K^{+}	0.019	0.003	0.003	0.000	0.014	0.017
vacancy	0.121	0.198	0.167	0.283	0.322	0.194
OH^{-}	3.753	3.991	3.971	4.000	3.916	3.902
F^{-}	0.247	0.009	0.029	0.000	0.084	0.098

Table 1. Selected EPMA analyses of detrital tourmaline.

microprobe. Gahnite is present in small amounts in all studied samples. The average ZnO concentrations range from 19.8 wt% to 41.1 wt%. On the eastern side of the HCM (Lublin area) the ZnO concentration is on average 34 wt%, while on the western side (Miechów area), it is less by about 5 wt%.

Garnet

Garnets are reasonably stable heavy minerals in burial diagenesis, with their stability, however, depending on chemical composition (Morton and Hallsworth 2007), and tend to be valuable minerals in provenance analysis (Biernacka and Józefiak 2009; Salata 2013; Krippner *et al.* 2014; Fleming *et al.* 2016; Dill and Škoda 2017). Garnets are found in most of the analysed samples, ranging from 0.5 to 52% (on average 13%) of all non-opaque heavy minerals. They occur mostly in the magnetic fraction in the size range from 63 μm to 250 μm. The garnet grains are angular, subangular, subrounded, and rounded (Text-fig. 8F). A degree of corrosion can be described as unweathered to the advanced stage (Andò *et al.* 2012). In some cases (Text-fig. 10),

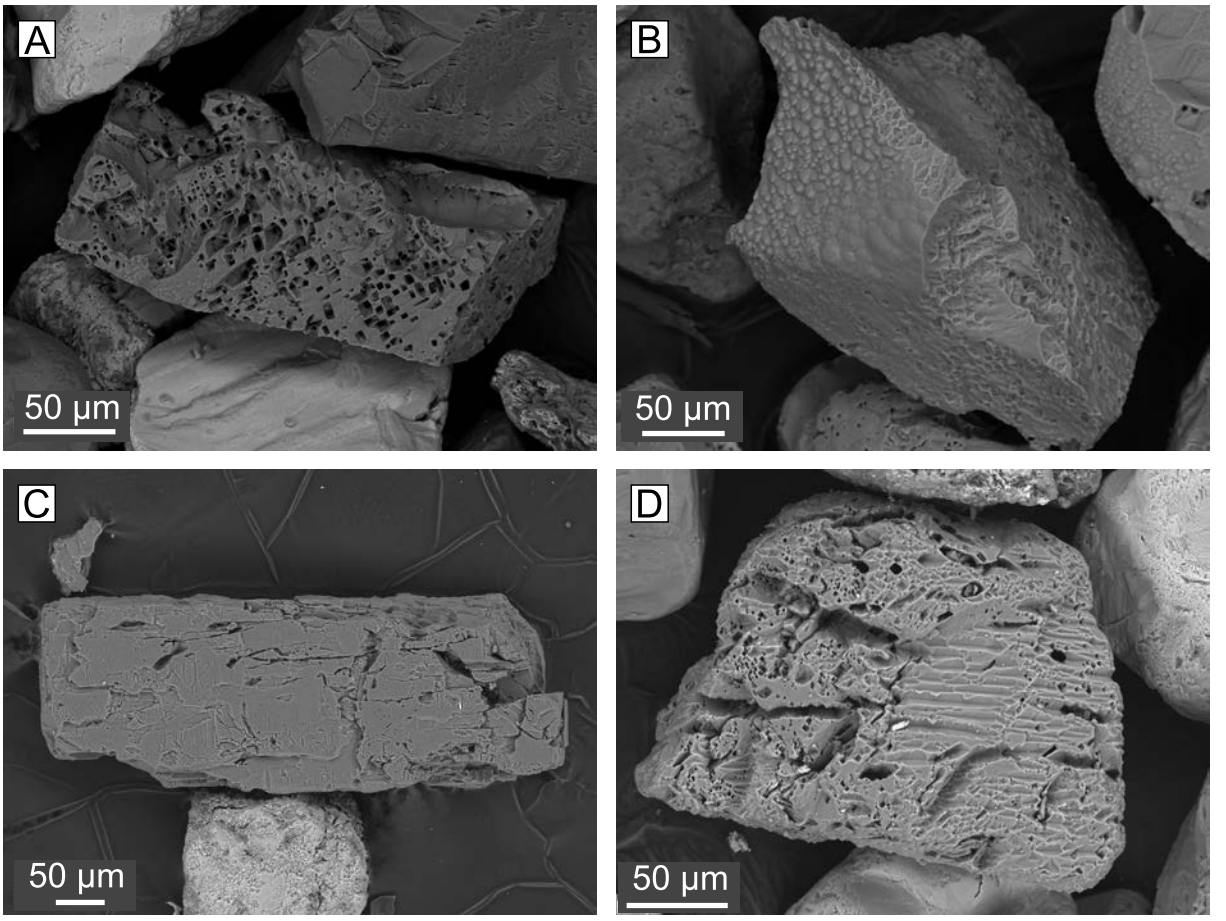

Text-fig. 10. SEM-BSE images of weathered heavy minerals. A – highly etched garnet from Glanów-Stroniczki; B – garnet with moderately etched, mamillated surface (compare Morton 1979) from Mokrzesz; C – etched kyanite from Mokrzesz; D – highly etched staurolite from Lelów.

they have a moderately and heavily etched crystal surface (compare Turner and Morton 2007; Velbel *et al.* 2007), or mamillated surfaces (compare Morton 1979). The chemical composition of the garnet population (Table 3) in the studied samples is dominated by almandine (approx. 67% of all garnet grains), pyrope (15%), and grossular (12%). Less common are spessartine (3%) and andradite (3%) (Text-fig. 11). The chemical composition of garnets in the eastern part of the study area (Lublin area) is relatively homogeneous. Almandine dominates (approx. 66%) and the rest of the garnets (grossular, pyrope, spessartine, andradite) occur in roughly similar proportions. In the samples from the western part (i.e., Miechów area), almandine also dominates (57%), but in comparison to the samples from the Lublin area, there is a greater proportion of pyrope (31%) and a smaller of grossular (10% in the Miechów area and 15% in the Lublin area) (Text-fig. 11).

Staurolite

Staurolite is a significant nesosilicate mineral indicating medium- and high-grade regional metamorphism (i.e., Barrovian metamorphism). Staurolite is present in all samples with a mean value of 5% of all transparent heavy mineral grains (Text-fig. 7). Most grains tend to concentrate in the 100–250 µm size fractions. Grains with a size of c. 300 µm can also be quite frequent (Text-fig. 8G). The surface of the majority of staurolite grains is visibly weathered (Text-fig. 10D), in some cases highly etched (compare Turner and Morton 2007). There is very little difference in chemical composition between the analysed staurolite grains. Most grains are typical Fe-rich staurolite with minor Mg and Zn constituents. Although Zn concentrations in the studied staurolite can reach up to 2 apfu, its mean value does not exceed 0.1 apfu (Table 4). The values of ferruginosity, i.e., $(Fe_{tot} + Mn)/(Fe_{tot} +$

Sample	Zn-spinel		Cr-spinel			
	Piaski 1,2A	MO ×3	LK ×36	GLA1_12	BOL_18	MO_65
Major constituents (wt%)						
SiO_2	bdl	bdl	bdl	0.10	bdl	0.03
TiO_2	0.14	0.03	0.77	1.99	0.22	0.13
Al_2O_3	54.44	57.73	12.97	26.71	16.70	25.91
$_{Cr2O3}$	2.26	0.34	51.88	32.16	52.88	43.61
FeO	6.12	11.96	5.80	22.98	19.23	17.62
MnO	0.17	0.25	6.20	0.23	0.25	0.26
NiO	–	–	bdl	0.15	bdl	bdl
MgO	2.00	2.64	4.70	14.60	10.13	12.05
ZnO	34.93	27.32	16.79	bdl	bdl	bdl
V_2O_3	0.08	0.08	0.11	0.29	0.20	0.24
Total	100.14	100.34	99.21	99.21	99.60	99.86
Calculated based on 3 cations (apfu)						
Si	0.000	0.000	0.000	0.003	0.000	0.001
Ti	0.003	0.001	0.020	0.045	0.005	0.003
Al	1.922	1.987	0.530	0.944	0.634	0.933
Cr	0.054	0.008	1.423	0.763	1.346	1.053
Fe	0.153	0.292	0.168	0.577	0.518	0.450
Mn	0.004	0.006	0.182	0.006	0.007	0.007
Ni	0.000	0.000	0.000	0.003	0.000	0.000
Mg	0.089	0.115	0.243	0.653	0.486	0.548
Zn	0.772	0.589	0.430	0.000	0.000	0.000
V	0.002	0.002	0.003	0.007	0.005	0.006
Total	3.000	3.000	3.000	3.001	3.000	3.000
#Mg	0.37	0.28	0.59	0.53	0.48	0.55
#Cr	0.03	0.00	0.73	0.45	0.68	0.53
#Zn	0.83	0.67	0.72	0.00	0.00	0.00

Table 2. Representative EPMA spinel analyses from Albian arenites. #Mg = Mg/(Mg+Fe^{2+}); #Cr = Cr/(Cr+Al); #Zn = Zn/(Zn+Fe^{2+}); bdl – below detection limit.

Mn + Mg), are similar between sample locations. The mean ferruginosity in staurolite grains is 0.84 in the Miechów area and 0.81 in the Lublin area.

Al_2SiO_5 polymorphs

The three Al_2SiO_5 nesosilicates (i.e., andalusite, kyanite, and sillimanite) are important metamorphic minerals indicating distinct metamorphic conditions in which they crystallise. The most common aluminosilicate is kyanite with only sporadic grains of sillimanite being noted. Despite the very good cleavage, the mineral appears quite often as a detrital component in various clastic rocks. In the studied material, the presence of kyanite was noticed at first under stereoscopic microscopy (Text-fig. 8H) and then confirmed by XRD analysis. The size of grains ranges from below 100 μm to over 300 μm. A degree of corrosion can be described as unweathered to slight stage, rarely advanced stage (Andò *et al.* 2012). The surface of grains is visibly etched (Text-fig. 10C) and eroded (Turner and Morton 2007), but a clear columnar/bladed crystal habit can still be recognised (Text-fig. 8H). In most cases, grains are colourless, but in some cases, a pale blue colour can be observed.

Fe-Ti oxides

Fe-Ti oxides occurring in the examined Albian siliciclastic deposits are represented by ilmenite and magnetite grains with different amounts of Ti (Text-fig. 12). Almost all Fe-Ti oxide grains revealed complex textures that originated during subsolidus oxy-exsolution processes (Haggerty 1976, 1991) which record their complex recrystallisation history during their evolution in the primary parent rock that constitutes the source area. The preserved textures of oxide intergrowths (Text-fig. 12F, G), despite their extensive breakdown into anatase during the diagenetic stage, still indicate their magmatic and metamorphic origins. All textural varieties of Fe-Ti oxides observed in the examined samples document their evolution in mafic (gabbro, amphibolite) through intermediate (andesite) to acidic (granitoid, gneiss)

Sample	GLA1_G_55	MO_A_67	KOP_6	LK 0.3_4	TL 0.3_38	TL 0.3_60
	GLA	MO	KOP	LK	TL	TL
Major constituents (wt%)						
SiO_2	36.43	39.28	38.42	37.33	38.68	37.76
TiO_2	0.41	bdl	0.06	0.24	0.13	0.38
Al_2O_3	20.17	22.16	20.62	20.29	20.67	20.28
FeO	1.15	25.30	24.24	34.57	31.41	33.92
MnO	38.05	0.62	4.98	1.87	0.55	1.58
MgO	0.30	9.60	3.42	3.27	7.39	4.40
CaO	2.99	3.16	8.31	2.39	0.93	1.35
Na_2O	0.24	bdl	bdl	bdl	bdl	bdl
Cr_2O_3	0.05	bdl	0.02	bdl	0.03	0.02
Total	99.78	100.12	100.07	99.95	99.80	99.68
Formula based on 12 oxygens and with Fe^{2+}/Fe^{3+} calculated assuming full site occupancy (apfu)						
Si	2.991	2.999	3.030	3.004	3.031	3.023
Ti	0.025	0.000	0.004	0.015	0.008	0.023
Al	1.951	1.994	1.917	1.924	1.909	1.914
Cr	0.003	0.000	0.001	0.000	0.002	0.001
Fe^{3+}	0.025	0.005	0.040	0.047	0.042	0.032
Fe^{2+}	0.054	1.611	1.559	2.280	2.016	2.239
Mn	2.646	0.040	0.332	0.127	0.036	0.107
Mg	0.037	1.093	0.402	0.392	0.863	0.525
Ni	0.000	0.000	0.000	0.000	0.000	0.000
Zn	0.000	0.000	0.000	0.000	0.000	0.000
Ca	0.263	0.259	0.703	0.206	0.078	0.116
Total	7.995	8.001	7.987	7.995	7.985	7.980
End member calculations						
Uv	0.00	0.00	0.00	0.00	0.00	0.00
Adr	0.01	0.00	0.02	0.02	0.02	0.02
Prp	0.01	0.36	0.13	0.13	0.29	0.18
Sps	0.88	0.01	0.11	0.04	0.01	0.04
Grs	0.07	0.08	0.21	0.05	0.00	0.02
Alm	0.01	0.54	0.50	0.74	0.65	0.72
Total	0.99	1.00	0.98	0.99	0.98	0.97

Table 3. Selected electron microprobe analyses of garnet; bdl – below detection limit.

rocks (by analogy with textural varieties of Fe-Ti oxides presented in Haggerty 1976, 1991).

The Fe-Ti oxide assemblage observed in the Albian samples is strongly altered (Text-fig. 12). Nearly all Fe-Ti oxide grains break down to form low-temperature TiO_2 group minerals (mainly anatase) (Text-fig. 12B–D, F), hematite (Text-fig. 12E), and maghemite (Text-fig. 12G, H). The growth of secondary anatase, hematite and maghemite reflects leucoxenisation and martitisation (Ramdohr 1975; Mücke and Bhadra Chaudhuri 1991; Mücke and Cabral 2005; Kinebuchi and Kyono 2021) that can take place during low-temperature evolution of rocks that constitute the source area (Kądziałko-Hofmokl *et al.* 2013). It can also occur during the weathering of Fe-Ti oxides contemporaneous with the deposition of clastic material and following diagenetic processes (Maxbauer *et al.* 2016). The degree of alteration varies from relatively almost unchanged grains (Text-fig. 12A, E, F), through grains with initial leucoxenisation (Text-fig. 12B, E), maghemitisation, and/or martitisation (Text-fig. 12G, H), to grains that form complete pseudomorphs of anatase after primary Fe-Ti oxides (Text-fig. 12C, D, F).

DISCUSSION

In the studied transparent heavy mineral assemblage, the ultrastable minerals (i.e., zircon, tourmaline, and rutile) are usually the most frequent (Text-fig. 7). Other heavy minerals present, such as monazite, kyanite, Cr- and Zn-spinel, are also relatively stable during burial diagenesis (Morton and Hallsworth 2007). Garnet and staurolite are present in variable quantities (Text-fig. 7) and often show

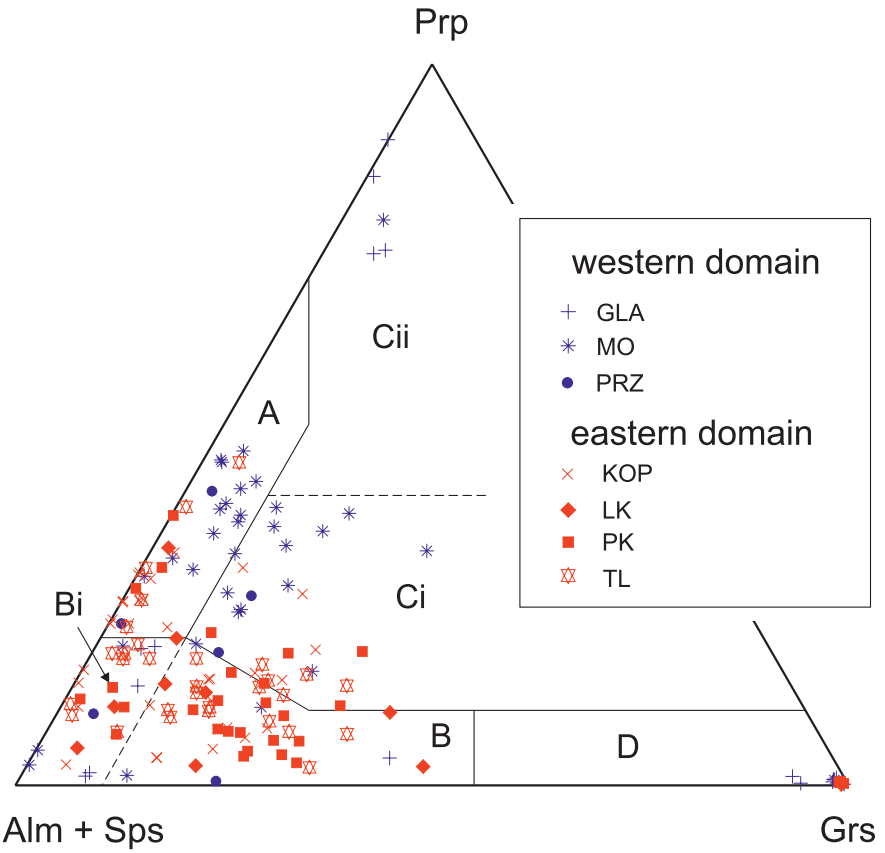

Text-fig. 11. Ternary discrimination diagram with molecular proportions of pyrope, almandine+spessartine, and grossular, after Mange and Morton (2007). A – high-grade granulite-facies metasediments or charnockites and intermediate felsic igneous rocks, B – amphibolite-facies metasedimentary rocks, Bi – intermediate to felsic igneous rocks, Ci – high-grade mafic rocks, Cii – ultramafics with high Mg concentrations, D – metasomatic rocks, very low-grade metamafic rocks and ultrahigh temperature metamorphosed calc-silicate granulites.

signs of significant chemical weathering. The substantial etch pits on garnet and staurolite surfaces (Text-fig. 10) may indicate an episode of acidic groundwater action before or after burial (Morton 1984; Velbel *et al.* 2007). It is worth noting that detrital apatite was not found in our study material. One possibility to explain this is the absence of apatite in the source rock. However, apatite is a common igneous and metamorphic accessory mineral found in e.g., syenites, granites, carbonatites, pegmatites, marbles, skarns, and can often be present in various clastic sediments (Morton and Hallsworth 2007; Flowerdew *et al.* 2020). The absence of apatite can also indicate a diagenetic dissolution episode in an acidic environment (Morton 1986; Bateman and Catt 2007), especially in a warm and humid climate, which was dominant in the Early Cretaceous (Fenner 2001; Wagstaff *et al.* 2013). The ZTR (zircon–tourmaline–rutile) index (Hubert 1962) is quite uniform across all samples, with few exceptions (Text-fig. 7) with a mean value of c. 70%. This indicates a significant chemical dissolution of less stable minerals, recycling of older clastic detrital material, and/or long transport. Chemical weathering is also visible on common rock-forming minerals like feldspar, quartz, and white mica.

The most valuable method in provenance studies of Albian arenites was the geochemical and geochronological investigation of selected heavy minerals. The comparison of the absolute ages of detrital monazite (chemical Th-U-total Pb isochron method, i.e., CHIME dating) and muscovite ($^{40}Ar/^{39}Ar$ dating) with the ages of crystalline massifs adjacent to the Polish Basin during the Albian shows that the western part of the southern periphery (i.e., present-day Miechów area) of the Polish Basin was sourced by the Bohemian Massif, whereas its eastern part (present-day Lublin area) was supplied mainly from the Baltic Shield (Kotowski *et al.* 2023). Therefore we have defined two main domains in the study area,

Sample	GLA1_34	GCHG 1.2	PRZ6 0.3	KRZx81	LK_25	Piaski_19
Major constituents (wt%)						
SiO_2	27.89	26.93	26.81	28.56	27.95	27.70
TiO_2	0.45	0.75	0.44	0.26	0.96	0.85
Al_2O_3	53.16	53.22	54.49	52.51	52.80	52.72
Cr_2O_3	0.03	0.08	0.02	0.04	0.05	0.04
FeO	7.35	11.67	14.53	9.24	13.90	13.76
MnO	0.37	0.19	0.14	0.52	0.16	0.19
MgO	1.77	1.24	1.31	02.07	1.69	1.61
ZnO	6.45	3.77	0.44	5.26	0.52	0.59
Na_2O	0.21	0.11	bdl	0.11	bdl	bdl
H_2O*	2.15	2.14	2.15	2.16	2.16	2.14
Total	99.83	100.09	100.33	100.73	100.18	99.61
Calculated based on 48 oxygens (apfu)						
Si	8.135	7.889	7.788	8.275	8.110	8.086
Ti	0.098	0.166	0.095	0.056	0.210	0.186
Al	18.280	18.379	18.665	17.938	18.060	18.139
Cr	0.006	0.018	0.006	0.010	0.011	0.008
Fe	1.794	2.858	3.530	2.240	3.372	3.360
Mn	0.092	0.046	0.033	0.127	0.039	0.048
Mg	0.771	0.542	0.569	0.894	0.732	0.702
Zn	1.389	0.816	0.095	1.126	0.110	0.127
Na	0.118	0.064	0.000	0.059	0.000	0.000
Total	30.683	30.778	30.781	30.725	30.645	30.655
ferruginosity	0.71	0.84	0.86	0.73	0.82	0.83

Table 4. Selected EPMA analyses of staurolite. * H_2O concentration calculated based on stoichiometry. Ferruginosity $(Fe_{tot} + Mn)/(Fe_{tot} + Mn + Mg)$; bdl – below detection limit.

which were sourced from different land masses: the western domain (related to the Miechów area) and the eastern domain (associated with the Lublin area; Kotowski *et al.* 2023). The results from rutile geothermometry (i.e., zircon in rutile – ZIR method) used earlier allowed us to divide the study area into three zones: western, central and eastern (Kotowski *et al.* 2021). The western and central parts distinguished by rutile mineral chemistry are in agreement with the western domain distinguished by monazite dating (Kotowski *et al.* 2023), and the eastern part distinguished by the ZIR geothermometer coincides with the eastern domain designated by monazite CHIME dating (Kotowski *et al.* 2023). The south of the Lublin region (sample TL) apart from Proterozoic monazite ages has a significant proportion of Variscan monazite, which crystallised probably in rocks of the Bohemian Massif (Kotowski *et al.* 2023). The northern part of the Miechów area (i.e., GCH, BOL, MO samples) has an admixture of rutile grains originating probably from the Baltic Shield apart from the dominant rutile from the Bohemian Massif. A preliminary geochronological study of zircons confirms the general division of our study area into the western and eastern domains and shows the limited influence of old zircons (>1 Ga) from the

Text-fig. 12. Photomicrographs of Fe-Ti oxides occurring in the heavy mineral associations from the Albian quartz arenites. All documented → oxide grains were taken from the Glanów-Stroniczki (GLA) sample. A, B – representative set of Fe-Ti oxide grains, parallel (A) and crossed (B) nicols; white arrows indicate the parts of strongly altered grains that consist of anatase (Ant); C, D – TiO_2 pseudomorph that mainly consist of anatase (Ant) after primary ilmenite (pIlm) and Ti-bearing magnetite (pMag), parallel (C) and crossed (D) nicols; E – Detrital magnetite (Mag) and ilmenite (Ilm) altered during synsedimentary and/or diagenetic processes; magnetite is replaced by secondary hematite (martite) along {111} planes (Hem); ilmenite is successively replaced by fine-grained Ti-oxides (anatase), forming a rim of leucoxene (LEU) around the unaltered ilmenite core; other Fe-Ti oxides form anatase pseudomorph (leucoxene) after ilmenite (pIlm) or Ti-bearing magnetite (pMag); F – Leucoxene pseudomorph after ilmenite (pIlm) and Ti-bearing magnetite (pMag); orientation of anatase crystals (Ant) records texture of oxy-exsolved ilmenite lamellae in Ti-bearing magnetite; G – Leucoxene (LEU) pseudomorphs after texturally varied ilmenite (pIlm) and Ti-bearing magnetite (pMag); in the centre, a large altered ilmenite grain (pIlm) with numerous lens-like exsolutions of hematite (now black lenses filled by gangue minerals), which were then dissolved (hematite) during hydrothermal or diagenetic alteration; optically homogeneous magnetite (Mag) grains bear subtle traces of maghemitisation processes; H – Altered grains of Fe-Ti oxides representing leucoxene (LEU) pseudomorph after ilmenite and magnetite (Mag) that break down to maghemite; in the centre, a partly altered ilmenite (Ilm) grain whose history of alteration is clearly related to syn-sedimentary and/or diagenetic processes.

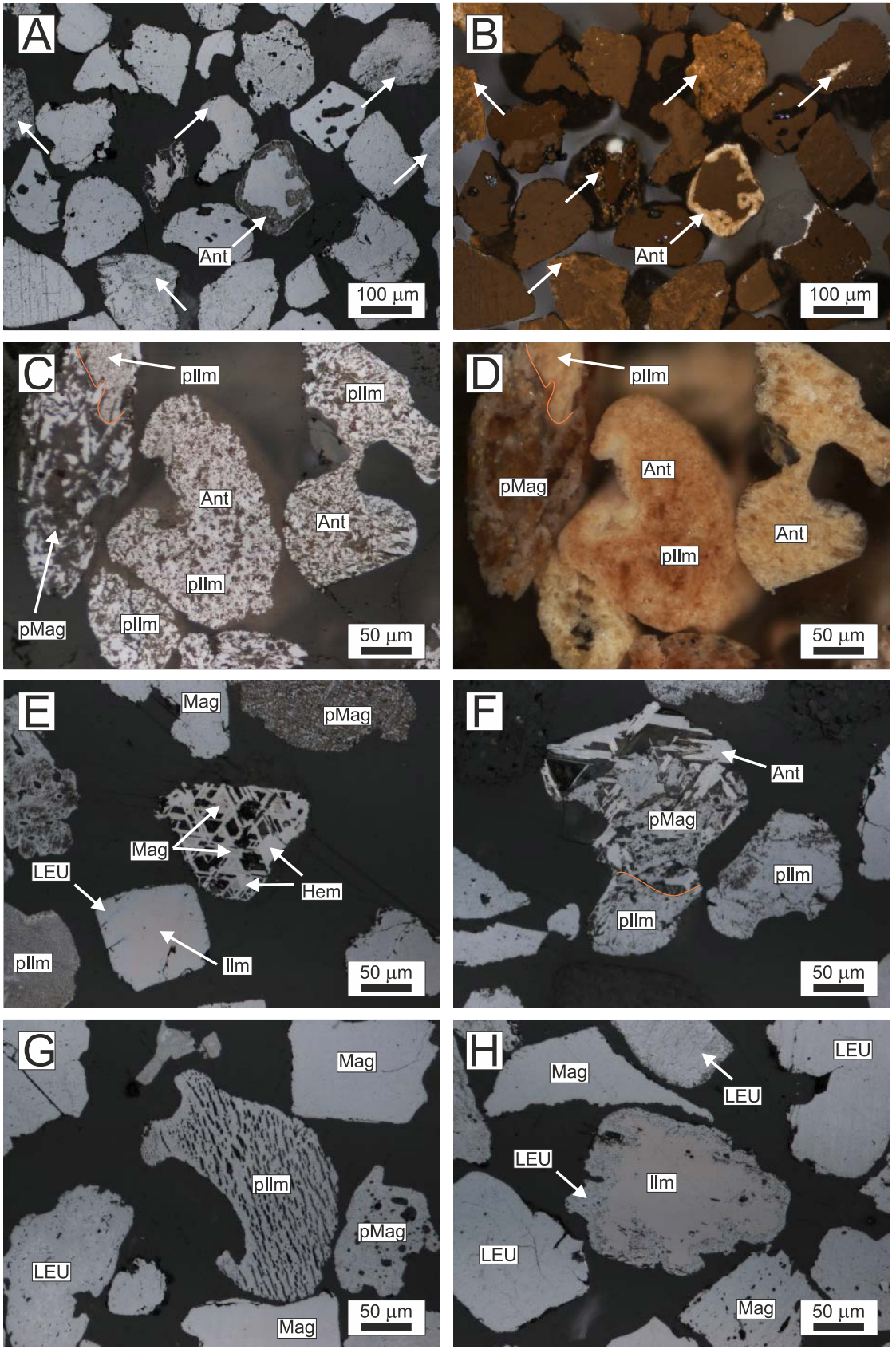
A
Ant
100 µm
B
Ant
100 µm
C
pIIm
pIIm
Ant
Ant
pIIm
pMag
pIIm
50 µm
D
pIIm
Ant
pMag
Ant
pIIm
50 µm
E
Mag
pMag
Mag
LEU
Hem
pIIm
Ilm
50 µm
F
Ant
pMag
pIIm
pIIm
50 µm
G
Mag
pIIm
pMag
LEU
Mag
50 µm
H
Mag
LEU
LEU
LEU
Ilm
LEU
Mag
50 µm

Baltic Shield to the northern part of the Miechów area (unpublished data).

The detrital tourmaline geochemistry was also quite informative. The chemical composition of tourmaline grains in the Fe-Al-Mg discriminant diagram in the Lublin area (the eastern group) is located chiefly in fields 4 and 5 related to metapellites and metapsammites, similar to the chemical composition of tourmaline grains from the Miechów area (the western group). Some grains from the western domain follow a diagonal trend towards field 2, i.e., Li-poor granitoid and their associated pegmatites and aplites (Text-fig. 9). Such discrimination in the western group suggests the influence of two or more different lithological sources of clastic material in the Miechów area. The diagonal trend is not visible in the eastern group and the densely grouped points on the diagram may indicate a single lithological source in the eastern group of tourmalines. The tourmalines from the western group are derived probably from the eastern part of the Bohemian Massif, most likely from rocks of the low and medium grade of metamorphism, i.e., mica schists and to a lesser extent gneisses (Kotowski *et al.* 2020). The 'eastern tourmalines' are derived, as we can suppose, from the same source as monazite, muscovite and rutile, i.e., mainly from the Baltic Shield source area.

The apparent division of the study area into two distinct main domains, described in previous papers (Kotowski *et al.* 2021, 2023), can be also traced in the chemical composition of other heavy mineral groups such as garnet and spinel.

The concentration of MgO, FeO_{tot}, CaO, Al_2O_3 and SiO_2 in garnet and the ratios between them (e.g., CaO to Al_2O_3) made it possible to distinguish garnet originating from metamorphic (MM; e.g., schists, metasediments), mantle (MA; e.g., pyroxenite, mafic xenoliths or eclogite), igneous (IG; e.g., granitoids, andesites, pegmatites), and metasomatic rocks (MS; e.g,. skarns) (Schönig *et al.* 2021). In all samples, metamorphic garnet (on average 71%) is dominant (Text-fig. 13). In the eastern domain, garnet of amphibolite facies and upper amphibolite/lower granulite facies predominates (Text-fig. 11). Most likely source rocks were metasedimentary rocks (e.g., schists), gneisses and amphibolites. Garnets from the Miechów area (i.e., western domain) crystallised mostly in conditions of granulite and eclogite facies. Nevertheless, some garnet grains from amphibolite facies are also present (Text-fig. 11). Dominant source rock types in this zone were most likely metasediments from high-grade granulite facies, gneisses and granulites (Aubrecht *et al.* 2009). Igneous garnet occurs in almost all samples; however, it is rare or absent in samples from the Miechów area but quite common in samples from the Lublin area. Mantle garnet is found only in samples from the Miechów area (Text-fig. 13). Metasomatic garnet appears in one sample from the Miechów area and two samples from the Lublin area. The amount of metasomatic garnet (MS) is strictly connected with the amount of CaO in the crystal structure. The Ca-rich garnets are most prone to dissolution during diagenesis (Morton and Hallsworth 2007), so their relative amount in sediment does not always correspond well with their source rock(s). Using the (Alm+Sps)-Prp-Grs discrimination diagram it was possible to notice a division between garnets originating from the eastern and western domains (Text-fig. 11). Garnets from the Miechów area (western domain) are concentrated mainly in fields corresponding to high-grade metamorphic, metasomatic, mafic, and ultramafic rocks, while garnets from the eastern domain tend to concentrate in fields equivalent to intermediate-grade (amphibolite

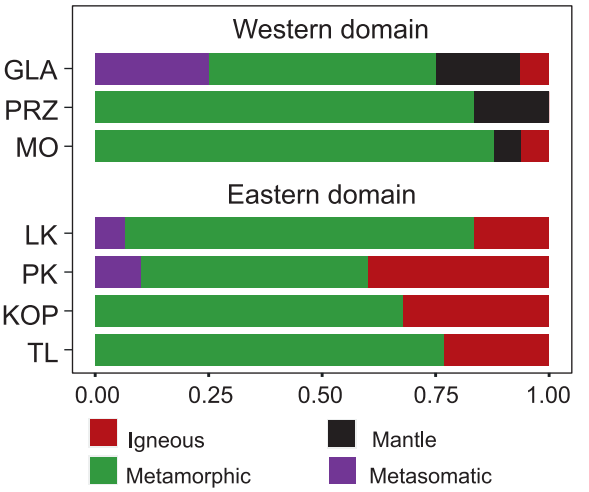

Text-fig. 13. Bar chart showing class assignment of garnets (after Schönig *et al.* 2021).

Text-fig. 14. Ternary plots of garnet from Albian arenites compared to the composition of garnet from rocks of: A – Sudetes – part of the Bohemian Massif (Biernacka and Józefiak 2009 and references therein), B – Sweden (Mannerstrand and Lundqvist 2003), C – Norway (Morton *et al.* 2004), D – sketch map of Norway showing sampled areas in C (N1–N6), modified after Morton *et al.* (2004). I – Strzegom-Sobótka granite; II – Góry Sowie Massif; III – Kamieniec Belt; IV – Doboszowice gneisses; V – Niemcza zone; VI – Orlica-Śnieżnik Dome; VII – Lusatian-Izera Massif; VIII – East-central Sweden; IX – South-west Sweden; X – Sjönevad, SW Sweden; XI – Tjörn, western Sweden; XII – Eftra, SW Sweden. →

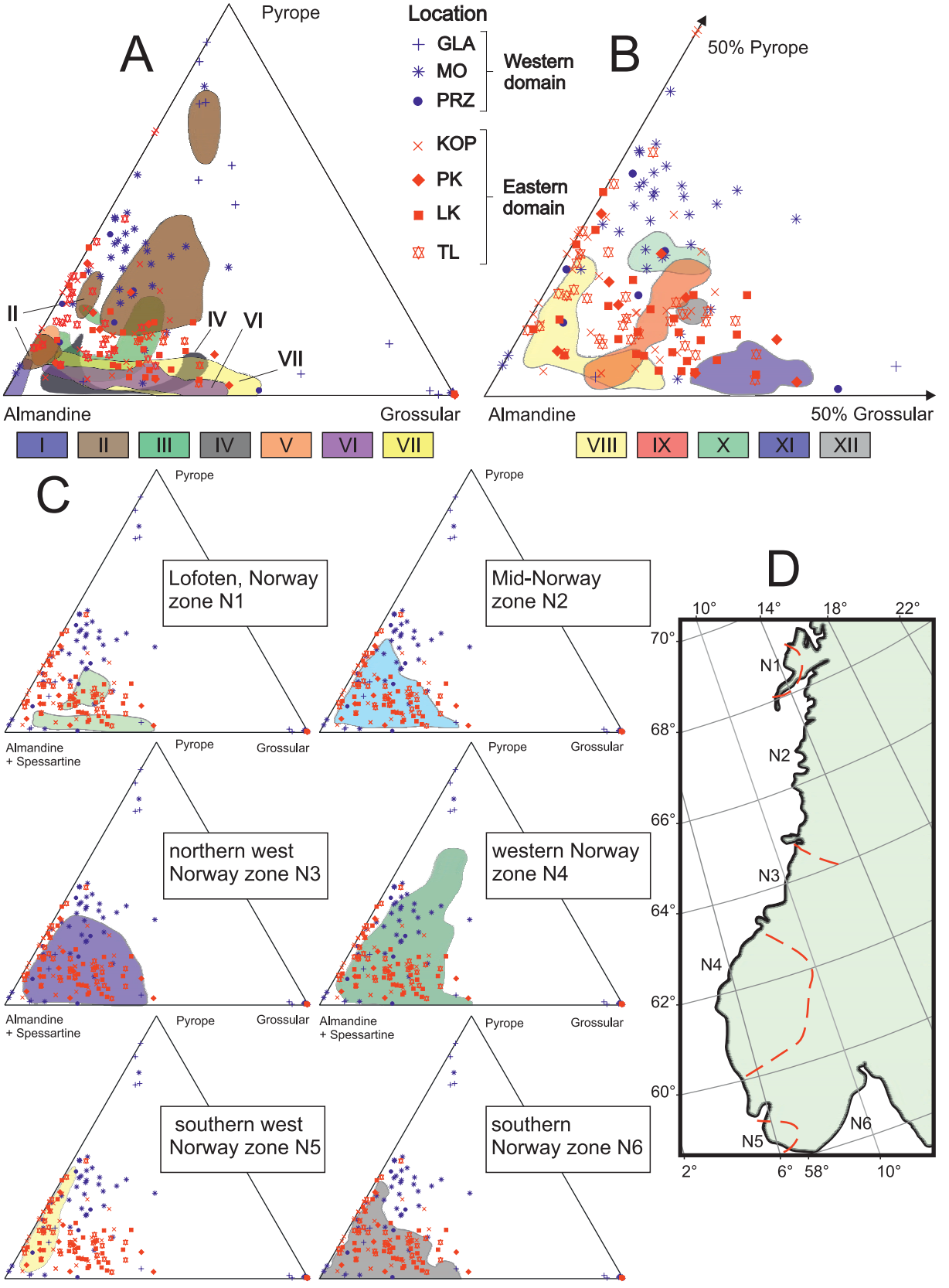
A
Pyrope
Almandine
Grossular
II
IV
VI
VII
Location
GLA
MO
PRZ
Western domain
KOP
PK
LK
TL
Eastern domain
B
50% Pyrope
Almandine
50% Grossular
I
II
III
IV
V
VI
VII
VIII
IX
X
XI
XII
C
Lofoten, Norway zone N1
Mid-Norway zone N2
northern west Norway zone N3
western Norway zone N4
southern west Norway zone N5
southern Norway zone N6
Pyrope
Grossular
Almandine + Spessartine
D
10°
14°
18°
22°
70°
68°
66°
64°
62°
60°
2°
6°
58°
10°
N1
N2
N3
N4
N5
N6

facies) metamorphic and igneous rocks (Text-fig. 11). However, the determination of sediment provenance based solely on garnet ratios can be subject to significant misinterpretations. This may be caused by the dissolution of less stable garnets by which the studied garnet assemblage may be different from that of source rocks. In the case of the studied Albian sediments this eventuality may be indicated by the high degree of chemical weathering observed on the garnet surface (Text-fig. 10A, B) and their relative scarcity in some samples. Nevertheless, some differences in the chemical composition of garnets seem to confirm various sources of origin in the Miechów and Lublin areas, similar to other heavy minerals. Garnets from the Miechów area, i.e., western domain, plotted on the discrimination diagram (Text-fig. 14A) show some similarities to garnets found in the Góry Sowie Massif (a part of the Sudetes). That part of the Sudetes was also thought to be the source of detrital tourmaline in Albian arenites from the Miechów area (Kotowski *et al*. 2020). However, the chemical composition of garnet from the Lublin area (eastern domain) is comparable to garnet from central and southern Norway (Text-fig. 14C) and is less correlated to garnet from Sweden (Text-fig. 14B). This may indicate a similar origin of the eastern domain garnets as some monazites, which were sourced from the Sveconorwegian rocks of southern Norway (Kotowski *et al.* 2023).

Chromium spinels (magnesiochromite $MgCr_2O_4$ and chromite $Fe^{2+}Cr_2O_4$) are common in mafic and ultramafic rocks and are frequently found in various sedimentary rocks (Mange and Wright 2007). Practically, Cr-spinels are most often the only minerals found in sedimentary rocks which were derived from mafic and ultramafic source rocks. Other minerals such as olivine, pyroxenes, and Ca amphiboles are relatively easily weathered and dissolved during diagenesis, so generally they are absent in most sedimentary rocks. The most susceptible elements in the structure of Cr-spinel to physicochemical changes during crystallisation are Al, Mg, and Fe; therefore, based on their ratios and contents, various discriminant diagrams were constructed (Mange and Wright 2007). Considering the Ti and Al content, most of the Cr-spinels from the western (BOL, GLA, KRZ, PRZ, LEL, MO, and GCH) and southern part of the eastern domain (TL) are characteristic of supra-subduction zone peridotites (SSZ) and MORB (Mid-Ocean Ridge Basalt) peridotite, while spinel grains from the northern part of the eastern domain (samples LK and PK) are split between the SSZ and island-arc basalts (Text-fig. 15). The difference is not very significant, but it is nonetheless noticeable. A more significant difference can be seen in the TiO_2 content in the LK and PK samples. These samples come from the boreholes located farthest to the northeast. The TiO_2 concentrations are more than two times higher than in the rest of the studied samples. This indicates at least a partial origin from rocks other than mantle peridotites. This, in turn, may imply a different source than the spinels from samples located in the southern parts of the study area or that there is at least a partial contribution from a different source of detrital material. Some researchers investigating the geotectonic origin of Cr spinels, however, question the validity of spinel geochemistry as a sole and precise provenance indicator (Power *et al.* 2000; Bónová *et al.* 2018).

Gahnite ($ZnAl_2O_4$) is much less common in the studied samples than its Cr counterpart. Using the plotted ratios: (Zn+Mn)/Al *vs.* (Fe^{2+}+Mg)/Al in Zn spinel, a division into western and eastern domains is evident (Text-fig. 16). Therefore it indicates different lithological types of source rocks in the abovementioned domains. Gahnite from the western part of the area (Miechów area) has a more metamorphic association while spinels from the eastern domain (Lublin area) tend to be associated to a greater degree with igneous rocks. The chemical composition of Cr and Zn spinels also confirms a distinctive source area for detrital minerals in the western and eastern domains. Although the division into two domains with different sources of clastic material is visible in the chemical composition of Zn spinel, a precise indication of specific crystalline massifs is very difficult.

Staurolite is a common heavy mineral in clastic sediments. However, it has not been widely used in provenance research so far. Its chemical composition does not change as much as in the case of garnet or tourmaline. There are no clear distinctions between staurolite grains from the eastern and western domains regarding their major element composition. It has been stated that 'ferruginosity', i.e., (Fe+Mn)/(Fe+Mn+Mg), is dependent on the metamorphism grade and could be used in provenance studies (Morton 1991). Yet the distribution of ferruginosity values of staurolites from the studied samples does not show significant variability between sampled locations. However, there is a slight shift in the ferruginosity towards lower values in the samples from the eastern domain (0.81) compared to the samples located in the western domain (0.84). The Zn content varies slightly between samples but does not correlate to the domain division. Overall, the chemical composition of staurolite does not provide a good discrimination between the studied samples.

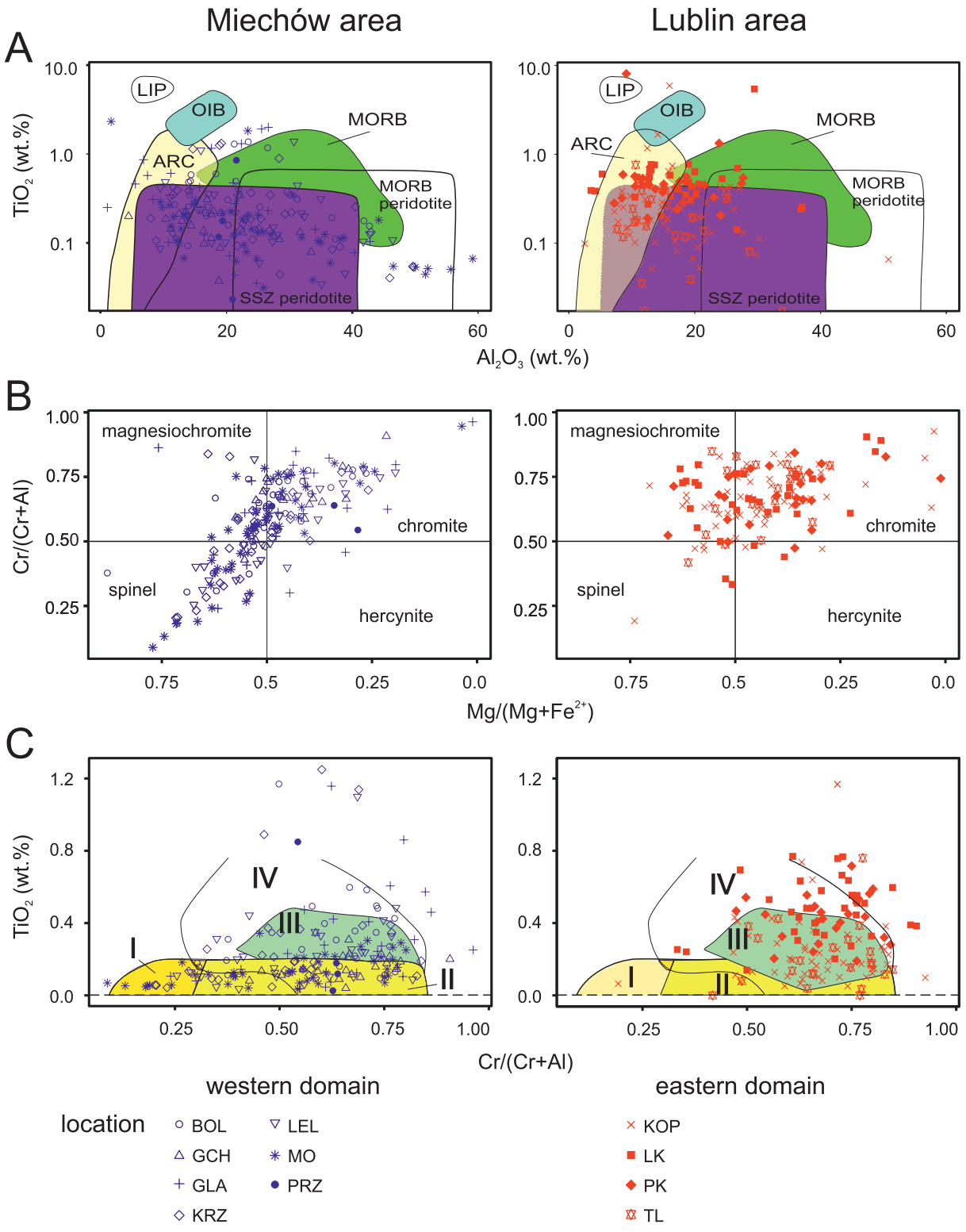

Text-fig. 15. Cr-spinel discrimination diagrams from the Miechów and Lublin areas. A – Al_2O_3 *vs.* TiO_2 compositional relationships in Cr-spinel after Kamenetsky *et al.* (2001). MORB (green) – Mid-Ocean Ridge Basalt; LIP (white) – Large Igneous Province; ARC (yellow) – island arc magmas; SSZ (violet) – Supra-Subduction Zone peridotite; OIB (blue) – ocean-island basalt . B – classification of the composition of chrome spinels after Schulze (2001); C – TiO_2 vs. Cr/(Cr+Al) diagram of spinels after Pober and Faupl (1988); I – lherzolites, II – harzburgites, III – podiform chromites, IV – ultramafic cumulates.

Nonetheless, the mere presence of staurolite may indicate the origin of initial source rocks as medium metamorphism (approx. amphibolite facies). The coexistence of staurolite with almandine and kyanite, which are also present in the samples, may indicate their common origin from rocks of the Barrovian metamorphism-type rocks (Deer *et al.* 1992), most likely pelitic schists.

Fe-Ti oxides subjected to even slight alterations during weathering and diagenesis rapidly change their chemical composition due to the oxidation of Fe, and diffusion of Mg, Mn, and Fe. In polarized reflected light, alteration processes can be easily noticed, and are expressed by a change in the colour of Fe-Ti oxides, inhomogeneity/submicroscopic granularity of the oxide surface, and the appearance of brown, yellow or white internal reflections, observed in the most strongly altered grains of Fe-Ti oxides (Text-fig. 12). Strong changes in the chemical composition recorded even in initially altered Fe-Ti oxides do not allow the use of the chemical composition of the oxides to analyse the provenance of detrital material.

The strong alteration of magmatic/metamorphic Fe-Ti oxides took place during weathering and diagenesis. Ilmenite and Ti-bearing magnetite are still further transformed into leucoxene pseudomorphs (Text-fig. 12), while magnetite is replaced by hematite (martite) or is continuously transformed into maghemite as a result of oxidation and diffusion of Fe (Ramdohr 1975; Haggerty 1976, 1991; Weibel and Friis 2007). During weathering and/or diagenesis, some of the oxides may undergo dissolution, which leads to the formation of open spaces usually filled with minerals that form a diagenetic cement in the sedimentary rock, and/or breakdown into diagenetically stable phases (Weibel and Friis 2007).

The orientation of secondary anatase and hematite helps distinguish the products of oxide transformations occurring in the source rocks and during sedimentological/diagenetic processes. Under conditions of weathering and diagenesis, the alterations of mineral associations are usually distributed as co-shaped to the grain boundaries (Text-fig. 12B, E, H) and have a more fine-grained texture. Alteration products of Fe-Ti oxides originated during subsolidus, metamorphic and hydrothermal stages are texturally more coarse-grained (Text-fig. 12F), than those developed during weathering or diagenesis (Text-fig. 12E, H). Additionally, cross-cutting relationships of detrital grain boundaries to aggregates of secondary Ti-minerals make it possible to distinguish diagenetic anatase (Text-fig. 12A, B, H; see leucoxene rims on ilmenite grains) from anatase that grows in crystalline rocks before their weathering (Text-fig. 12E; see altered magnetite grain in the centre of the microphotograph).

The alterations of Fe-Ti oxides documented in the quartz arenites correlate very well with the dissolution processes of other detrital heavy minerals, such as garnet, kyanite, or staurolite. During these alterations, the crystallization of kaolinite group minerals occurred at the expense of muscovite and feldspars. The transformation processes of Fe-Ti oxides are also most likely related to the lack of minerals, e.g., apatite, that are unstable during weathering and diagenesis.

Summarising, in this study of the provenance of the Albian arenites in the southern part of the Polish Basin, the most important are geochronological studies, i.e., monazite (CHIME) and muscovite ($^{40}Ar/^{39}Ar$) dating (Kotowski *et al.* 2023). They give a good description of the source areas of crystalline massifs located in the vicinity of the study area. Therefore, it was possible to deduce the directions of transport of the clastic material mainly from two crystalline massifs: from the Bohemian Massif to the Miechów area and from the Baltic Shield to the Lublin area. Rutile mineral chemistry gave insight into the crystallisation temperature conditions and lithology from which those detrital rutile originated (Kotowski *et al.* 2021). Similarly, the chemistry of tourmaline (Kotowski *et al.* 2020), spinel and garnet grains allowed us to infer the lithology from which specific minerals were sourced. It is important to note that source lithology deduced from each of the analysed heavy minerals may differ. Detrital tourmaline and rutile may probably have come from different rock types (e.g., mica schist and mafic or ultramafic rocks, respectively). It is important to look at the whole heavy mineral assemblage to deduce the most probable area of provenance.

While source areas of detrital material in Albian clastic sediments were recognised in both domains, the intermediate sources are not well defined. Euhedral grains and unweathered surfaces of selected heavy minerals may indicate their origin in crystalline massifs. The lack of significant sub-Upper Albian clastic deposits on lands during the Late Albian also implies a first cycle sediment. However, several detrital grains have visibly weathered surfaces which may indicate either recycled material or significant alterations during burial diagenesis. On some detrital quartz grains, abraded overgrowths are also noted. The presence of weathered quartz overgrowths unequivocally indicates a recycled material from older sediments (Basu *et al.* 2013).

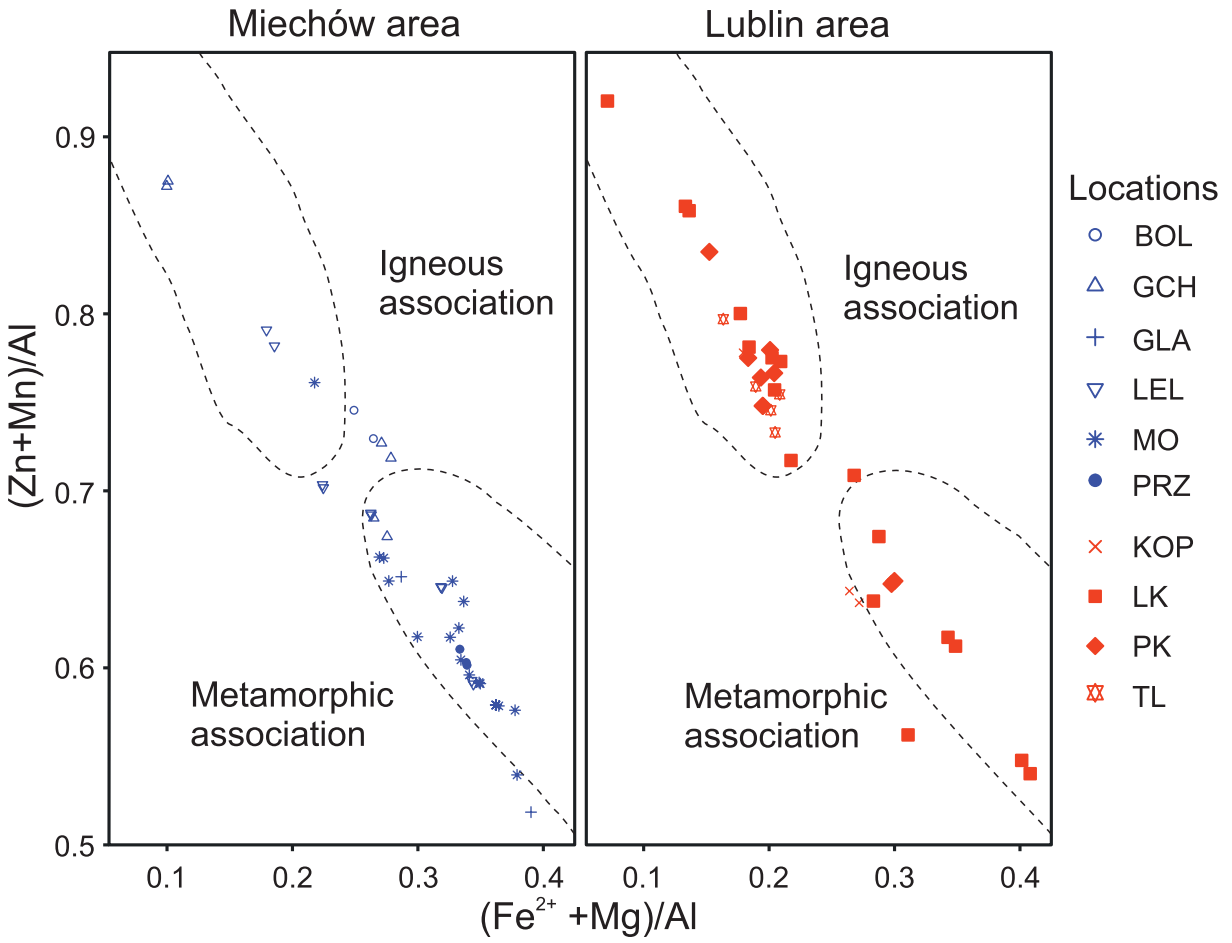

Text-fig. 16. Bivariate plot (Zn+Mn)/Al *vs.* (Fe+Mg)/Al of Zn-spinel from the Miechów and Lublin areas on the Batchelor and Kinnaird (1984) discrimination diagram.

During the Albian, the extra-Alpine epicontinental areas of Europe were flooded by the sea constituting the Central European Basin System (CEBS). The Polish Basin was situated in the eastern part of the CEBS. The sea transgressed onto the land area of mainly Jurassic substrate built of various limestones, marly limestones or marls. It is confirmed by Jurassic cherts and carbonate lithic fragments in the Albian samples and by the presence of basal conglomerates and a smoothed-out abraded surface of Jurassic limestones with animal borings (e.g., sponges, bivalves, worms, gastropods). In a few places, the substrate for the Albian transgression is built of Lower Cretaceous, pre-Albian fine-grained sediments (Marek 1988, Leszczyński 1997) or Carboniferous siltstones, mudstones, and sandstones in the easternmost parts of Poland (Krassowska 1976). The Jurassic carbonate substrate is not a good reservoir for detrital quartz material, which is the main component of the Albian arenites. Lower Cretaceous and Carboniferous very fine-grained sandstones, mudstones, siltstones, and claystones could not be the main source for fine- and medium-grained Albian arenites. Carboniferous deposits, on which the Cretaceous sea had encroached, are of very limited exposure (i.e., restricted only to the easternmost parts of Poland) and are built mainly of various fine-graded clastic sediments. Similarly, Lower Cretaceous deposits were also restricted to the Mid Polish Trough (Leszczyński 1997) which makes them unlikely to be the main source of clastic material of Albian arenites.

The Albian arenites from southern Poland represent clastic shallow-marine and beach facies (Marcinowski 1974; Hakenberg and Świdrowska 2001; Olszewska-Nejbert *et al.* 2020). The detrital material might have been transported either directly from crystalline rocks and/or from older clastic rocks located in their vicinity, but containing detrital mate-

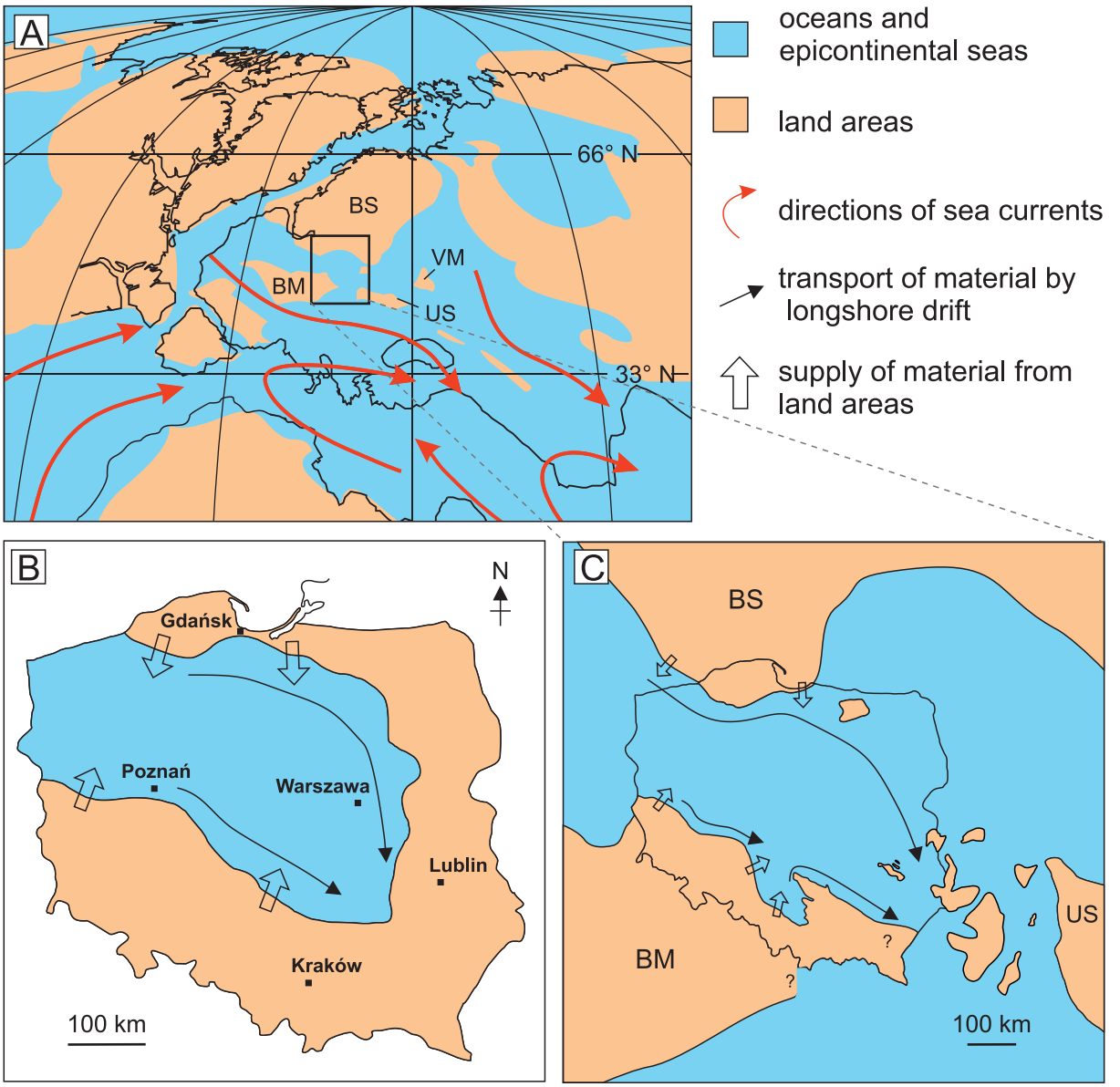

Text-fig. 17. Palaeogeographic maps: A – Ocean circulation simulation at c. 100 Ma (mid-Cretaceous – earliest Cenomanian) after Hay (2009). B – Palaeogeographic map of Poland during the Middle Albian (after Marek 1988, simplified), before the Late Albian transgression. C – Palaeogeography of Poland and surroundings in the Late Albian (modified after Jaskowiak-Schoeneichowa and Krassowska 1988; Ziegler 1988, 1990; Świdrowska *et al.* 2008); BM – Bohemian Massif, BS – Baltic Shield, US – Ukrainian Shield, VM – Voronezh Massif.

rial from them. The closest crystalline massifs with detrital sedimentary covers that are adjacent to the Polish Basin are the Bohemian Massif to the west, the Ukrainian Massif to the east, and the Baltic Shield further to the north. These areas, uplifted and rejuvenated during various tectonic movements, probably underwent erosion and appear to be the most probable source of the detrital material for Albian arenites. The origin of detrital material from crystalline massif(s) or older clastic rocks located further away is evidenced by weathered rare granitic lithoclasts, fragments of large (> 1mm) potassium feldspars (e.g., microcline and orthoclase), and quartzite fragments. The lithic grains and clasts, especially metamorphic and magmatic extraclasts are useful in provenance interpretations (Garzanti and Vezzoli 2003; Garzanti 2019). In our study lithoclasts are very rare. Moreover, a part of them are intraclasts (Text-fig. 6D, F), e.g.,

silicified wood and phosphorites. These intraclasts indicate only intrabasinal processes of silification and phosphatisation of the fossil remains. Cherts found in most studied samples may have come from eroded Jurassic carbonates that covered most land areas in the Albian (Hakenberg 1986). Fragments of sandstones and mudstones found in Albian arenites were most likely derived from a sedimentary cover overlying the Jurassic carbonate land areas. These clastic rocks could be eroded from lands during the Albian transgression. The observed lithoclasts of older rocks, such as fragments of granites, gneisses and quartz schists are present in the samples on the eastern and western sides of the HCM. In the case of the Albian arenites of southern extra-Carpathian Poland, such lithoclasts are not precise indicators of the source area, because similar rock types are common in the Bohemian Massif, the Baltic Shield, and also the Ukrainian Shield. In our study, the chemical analysis of HMs gave more precise conclusions regarding the source areas.

The chemical composition of heavy minerals from the Miechów area confirms the large influence of the Bohemian Massif on this part of the Polish Basin. However, material from the Bohemian Massif had a limited influence on the Lublin area, the more easterly part of the Polish Basin. In the vicinity of Tomaszów Lubelski, the southernmost part of the Lublin area, apart from the material from the Baltic Shield a significant influence of the Bohemian Massif is recorded. This is most probably caused by the action of longshore drift of mainly eastward direction along the southern shore of the Polish Basin in the Albian (Text-fig. 17). Moreover, during Albian times, the Ukrainian Shield, the nearest land to our study area, also did not provide clear evidence of the origin of detrital material from that direction. Heavy minerals in the Lublin area, meanwhile, indicate source rocks located in the Baltic Shield. Especially, the CHIME age of monazite grains shows distinctive 'fingerprint' ages, i.e., Sveconorwegian – 1 Ga (Bingen *et al.* 2021), and Caledonian – approx. 460–490 Ma (Barnes *et al.* 2022) characteristic of the Baltic Shield. Therefore, long transport of clastic material was possible thanks to longshore drift generated by the southeastward longshore current, from the general direction of the Baltic Shield to the south and east (Kotowski *et al.* 2023). This direction coincides well with the simulated sea currents circulation in the mid-Cretaceous (c. 100 Ma) oceans, compiled by Hay (2009). In and near the Tethys Ocean, i.e., to the south, close to our study area, the directions of currents are assumed to have been southeasterly (Text-fig. 17). This may also explain the lack of minor amounts of detrital material from the Ukrainian Shield, as that material might have been transported further away in the opposite direction to the Lublin area (i.e., southeastwards).

Based on the facies distribution in the Late Albian there was probably no significant land area(s) between the western and eastern domains (Świdrowska *et al.* 2008). In the vicinity of Annopol a zone known as the Vistula threshold or the Annopol swell (Cieśliński 1976; Walaszczyk 1987) was being uplifted in the Early Cretaceous, marking an area of shallows and periodic breaks in deposition. This uplifted area may have additionally influenced the directions of longshore currents and the transport of clastic material in a general eastward/southeastward direction.

The amount of clastic material supplied from eroded lands to the marine basin may have also been controlled by the relief of the eroded area and river drainage (e.g., Garzanti *et al.* 2010, 2019). In the Early Cretaceous, both the Bohemian Massif (Ventura and Lisker 2003) and the southern part of the Baltic Shield (Japsen *et al.* 2016) were areas of relatively varied relief elevated above sea level and subjected to erosion. In contrast, the area of the Ukrainian Shield being part of the East European Craton was not subject to any significant orogenesis in the Phanerozoic. Palaeozoic and Mesozoic sediments lie practically flat on the Precambrian (Bogdanova *et al.* 2016). It might be assumed that the Ukrainian Shield area was not differentiated hypsometrically and strongly peneplained. The Lower Cretaceous terrestrial sedimentary cover developing in the area of the Ukrainian Shield consisted mainly of kaolin clays and coarser clastic sedimentary rocks (Kroshko and Koval'chuk 2017).

CONCLUSIONS

Using variations in chemical composition in selected heavy minerals, it was possible to characterise the different provenance of Albian clastic material in the southern part of the Polish Basin. Each of the studied heavy minerals gives some information about the source area of Albian arenites.

The division of the study area into the western and eastern domains, fed by two different sources, i.e., the Bohemian Massif and the Baltic Shield, respectively, based on the CHIME (monazite) and $^{40}Ar/^{39}Ar$ (muscovite) geochronological data and mineral chemistry of rutile, is also recorded by mineral chemistry of tourmaline, garnet, and Zn- and Cr-spinel.

Tourmaline geochemistry indicates that the main source in both domains were medium-grade metamorphic rocks. In the western domain, tourmalines additionally may have been eroded from granitoids or gneisses. Most of the detrital garnets also indicate a prevalence of metamorphic rocks as the source lithology. In the eastern domain, there is also a noticeable number of igneous garnets, less prevalent in the western domain. Furthermore, garnets of mantle origin are present only in the western domain. The garnet from the western domain was derived most probably from the Sudetes, while the garnet from the eastern domain was sourced most likely from the southern and/or central parts of Norway. Mineral chemistry of Zn- and Cr-spinels also allows for the division of the study area into two domains with different sources of clastic material.

The apparent division of the study area into two domains of different provenance of clastic material was most probably the result of the palaeogeography of the region in the Early Cretaceous. The direction of longshore currents transporting large amounts of clastic material was mainly southeastward from the Baltic Shield to the Lublin area and generally eastward from the Bohemian Massif to the Miechów area.

Acknowledgements

The authors are greatly indebted to Jan Nowak, owner of the quarry near the Chełmo Mount, for permission to conduct this scientific investigation. The warmest thanks are offered to Petras Jokubauskas and Beata Marciniak-Maliszewska for help with EPMA investigations, and to Raymond Macdonald for linguistic correction. Special thanks go to Sergio Andò, Krzysztof Leszczyński and an anonymous reviewer for critical reviews and a lot of helpful comments and remarks. We also want to thank Anna Żylińska, the journal editor, for fruitful remarks, language corrections and kind help with editorial matters. This work was supported by the University of Warsaw, Faculty of Geology, Cryo-SEM Laboratory: National Multidisciplinary Laboratory of Functional Nanomaterials NanoFun project no. POIG.02.02.00-00-025/09. Support from the analytical facilities of the project RPO-WM 2007-2013 'Modernization and equipment supplement of laboratories at Faculty of Geology, University of Warsaw, for crucial environmental geo-engineering research and development of Mazovia: Stage 1' is acknowledged.

REFERENCES

Akdoğan, R., Okay, A.I., Sunal, G., Tari, G., Meinhold, G. and Kylander-Clark, A.R.C. 2017. Provenance of a large Lower Cretaceous turbidite submarine fan complex on the active Laurasian margin: Central Pontides, northern Turkey. *Journal of Asian Earth Sciences*, **134**, 309–329.

Andò, S., Garzanti, E., Padoan, M. and Limonta, M. 2012. Corrosion of heavy minerals during weathering and diagenesis: A catalog for optical analysis. *Sedimentary Geology*, **280**, 165–178.

Aubrecht, R., Méres, Š., Sýkora, M. and Mikuš, T. 2009. Provenance of the detrital garnets and spinels from the Albian sediments of the Czorsztyn Unit (Pieniny Klippen Belt, Western Carpathians, Slovakia). *Geologica Carpathica*, **60**, 463–483.

Barnes, C.J., Bukała, M., Callegari, R., Walczak, K., Kooijman, E., Kielman-Schmitt, M. and Majka, J. 2022. Zircon and monazite reveal late Cambrian/early Ordovician partial melting of the Central Seve Nappe Complex, Scandinavian Caledonides. *Contributions to Mineralogy and Petrology*, **177**, 92.

Basu, A., Schieber, J., Patranabis-Deb, S. and Dhang, P.C. 2013. Recycled detrital quartz grains are sedimentary rock fragments indicating unconformities: Examples from the Chhattisgarh Supergroup, Bastar craton, India. *Journal of Sedimentary Research*, **83**, 368–376.

Batchelor, R.A. and Kinnaird, J.A. 1984. Gahnite compositions compared. *Mineralogical Magazine*, **48**, 425–429.

Bateman, R.M. and Catt, J.A. 2007. Provenance and palaeoenvironmental interpretation of superficial deposits, with particular reference to post-depositional modification of heavy mineral assemblages. In: Mange, M.A. and Wright, D.T. (Eds), Heavy minerals in use, 151–188. Elsevier B.V.; Amsterdam.

Biernacka, J. and Józefiak, M. 2009. The eastern Sudetic Island in the early-to-middle Turonian: evidence from heavy minerals in the Jerzmanowice sandstones, SW Poland. *Acta Geologica Polonica*, **59**, 545–565.

Bingen, B., Viola, G., Möller, C., Vander Auwera, J., Laurent, A. and Yi, K. 2021. The Sveconorwegian orogeny. *Gondwana Research*, **90**, 273–313.

Blott, S.J. and Pye, K. 2001. Gradistat: A grain size distribution and statistics package for the analysis of unconsolidated sediments. *Earth Surface Processes and Landforms*, **26**, 1237–1248.

Bogdanova, S.V., Gorbatschev, R. and Garetsky, R.G. 2016. EUROPE|East European Craton. Reference Module in Earth Systems and Environmental Sciences, 1–18. Elsevier.

Bónová, K., Mikuš, T. and Bóna, J. 2018. Is Cr-spinel geochemistry enough for solving the provenance dilemma? Case study from the Palaeogene sandstones of the Western Carpathians (Eastern Slovakia). *Minerals*, **8**, 543.

Chlebowski, R., Hakenberg, M. and Marcinowski, R. 1978. Albian ammonite fauna from the Chełmowa Mt near Przedbórz (central Poland). *Bulletin de l'Academie Polonaise des Sciences*, *Serie des Sciences de la Terre*, **25**, 91–97.

Cieśliński, S. 1976. Development of the Danish-Polish Furrow in the Góry Świętokrzyskie region in the Albian, Cenomanian and Lower Turonian. *Biuletyn Państwowego Instytutu Geologicznego*, **295**, 249–271. [In Polish with English summary]

Dadlez, R. 2003. Mesozoic thickness pattern in the Mid-Polish Trough. *Geological Quarterly*, **47**, 223–240.

Dadlez, R., Grad, M. and Guterch, A. 2005. Crustal structure below the Polish Basin: Is it composed of proximal terranes derived from Baltica? *Tectonophysics*, **41**, 111–128.

Dadlez, R., Marek, S. and Pokorski, J. 2000. Geological map of Poland without Cenozoic deposits in the scale 1:1 000 000. Państwowy Instytut Geologiczny; Warszawa.

Deer, W.A., Howie, R.A. and Zussman, J. 1992. An introduction to the rock-forming minerals, 495 pp. Mineralogical Society of Great Britain and Ireland; Hertfordshire.

Dill, H.G. and Škoda, R. 2017. Provenance analysis of heavy minerals in beach sands (Falkland Islands/Islas Malvinas) – A view to mineral deposits and the geodynamics of the South Atlantic Ocean. *Journal of South American Earth Sciences*, **78**, 17–37.

Fenner, J. 2001. Middle and Late Albian geography, oceanography, and climate and the setting of the Kirchrode I and II borehole sites. *Palaeogeography*, *Palaeoclimatology*, *Palaeoecology*, **174**, 5–32.

Fleming, E.J., Flowerdew, M.J., Smyth, H.R., Scott, R.A., Morton, A.C., Omma, J.E., Frei, D. and Whitehouse, M.J. 2016. Provenance of Triassic sandstones on the southwest Barents Shelf and the implication for sediment dispersal patterns in northwest Pangaea. *Marine and Petroleum Geology*, **78**, 516–535.

Flowerdew, M.J., Fleming, E., Morton, A.C., Frei, D., Chew, D.M. and Daly, J.S. 2020. Assessing mineral fertility and bias in sedimentary provenance studies: examples from the Barents Shelf. *Geological Society of London*, *Special Publications*, **484**, 255–274.

Garzanti, E. 2017. The maturity myth in sedimentology and provenance analysis. *Journal of Sedimentary Research*, **87**, 353–365.

Garzanti, E. 2019. Petrographic classification of sand and sandstone. *Earth-Science Reviews*, **192**, 545–563.

Garzanti, E. and Andò, S. 2007a. Heavy mineral concentration in modern sands: implications for provenance interpretation. In: Mange, M.A. and Wright, D.T. (Eds), Heavy minerals in use, 517–545. Elsevier B.V.; Amsterdam.

Garzanti, E. and Andò, S. 2007b. Plate tectonics and heavy mineral suites of modern sands. In: Mange, M.A. and Wright, D.T. (Eds), Heavy minerals in use, 741–763. Elsevier B.V.; Amsterdam.

Garzanti, E., Andò, S., France-Lanord, C., Vezzoli, G., Censi, P., Galy, V. and Najman, Y. 2010. Mineralogical and chemical variability of fluvial sediments. 1. Bedload sand (Ganga-Brahmaputra, Bangladesh). *Earth and Planetary Science Letters*, **299**, 368–381.

Garzanti, E., Vermeesch, P., Vezzoli, G., Andò, S., Botti, E., Limonta, M., Dinis, P., Hahn, A., Baudet, D., De Grave, J. and Yaya, N.K. 2019. Congo River sand and the equatorial quartz factory. *Earth-Science Reviews*, **197**, 102918.

Garzanti, E. and Vezzoli, G. 2003. A classification of metamorphic grains in sands based on their composition and grade. *Journal of Sedimentary Research*, **73**, 830–837.

Gurba, L. 1984. Dokumentacja wynikowa otworu wiertniczego Piaski IG-2. Unpublished report, 23 pp. Archives of the Polish Geological Institute; Warszawa.

Haggerty, S.E. 1976. Oxide minerals. In: Rumble, D. (Ed.), Oxide minerals, 303–502. De Gruyter; Berlin.

Haggerty, S.E. 1991. Oxide textures; a mini-atlas. *Reviews in Mineralogy and Geochemistry*, **25**, 129–219.

Hakenberg, M. 1978. Albian–Cenomanian palaeotectonics and palaeogeography of the Miechów Depression, northern part. *Studia Geologica Polonica*, **58**, 8–104. [In Polish with English summary]

Hakenberg, M. 1986. Albian and Cenomanian in the Miechów Basin (Central Poland). *Studia Geologica Polonica*, **86**, 57–85. [In Polish with English summary]

Hakenberg, M., Jurkiewicz, H. and Woiński, J. 1973. Profiles of Middle Cretaceous in the northern part of the Miechów Trough. *Geological Quarterly*, **17**, 763–786. [In Polish with English summary]

Hakenberg, M. and Świdrowska, J. 2001. Cretaceous basin evolution in the Lublin area along the Teisseyre-Tornquist Zone (SE Poland). *Annales Societatis Geologorum Poloniae*, **71**, 1–20.

Hay, W.W. 2009. Cretaceous oceans and ocean modeling. In: Hu, X., Wang, C., Scott, R.W., Wagreich, M. and Jansa, L. (Eds), Cretaceous oceanic red beds: stratigraphy, composition, origins, and paleoceanographic and paleoclimatic significance, 243–271. SEPM Society for Sedimentary Geology; Tulsa.

Henry, D.J. and Guidotti, C.V. 1985. Tourmaline as a petrogenetic indicator mineral – an example from the staurolite-grade metapelites of NW Maine. *American Mineralogist*, **70**, 1–15.

Hubert, J.F. 1962. A zircon-tourmaline-rutile maturity index and the interdependence of the composition of heavy mineral assemblages with the gross composition and texture of sandstones. *Journal of Sedimentary Research*, **32**, 440–450.

Japsen, P., Green, P.F., Bonow, J.M. and Erlström, M. 2016. Episodic burial and exhumation of the southern Baltic Shield: epeirogenic uplifts during and after break-up of Pangaea. *Gondwana Research*, **35**, 357–377.

Jaskowiak-Schoeneichowa, M. and Krassowska, A. 1988. Palaeothickness, lithofacies and palaeotectonics of the epicontinental Upper Cretaceous in Poland. *Geological Quarterly*, **32**, 177–198. [In Polish with English summary]

Kamenetsky, V.S., Crawford, A.J. and Meffre, S. 2001. Factors controlling chemistry of magmatic spinel: An empirical

study of associated olivine, Cr-spinel and melt inclusions from primitive rocks. *Journal of Petrology*, **42**, 655–671.

Kądziałko-Hofmokl, M., Szczepański, J., Werner, T., Jeleńska, M. and Nejbert, K. 2013. Paleomagnetism and magnetic mineralogy of metabasites and granulites from Orlica-Śnieżnik Dome (Central Sudetes). *Acta Geophysica*, **61**, 535–568.

Kinebuchi, I. and Kyono, A. 2021. Study on magnetite oxidation using synchrotron X-ray diffraction and X-ray absorption spectroscopy: Vacancy ordering transition in maghemite (γ-Fe_2O_3). *Journal of Mineralogical and Petrological Sciences*, **116**, 211–219.

Kotowski, J., Nejbert, K. and Olszewska-Nejbert, D. 2020. Tourmalines as a tool in provenance studies of terrigenous material in extra-Carpathian Albian (uppermost Lower Cretaceous) sands of Miechów Synclinorium, Southern Poland. *Minerals*, **10**, 917.

Kotowski, J., Nejbert, K. and Olszewska-Nejbert, D. 2021. Rutile mineral chemistry and Zr-in-rutile thermometry in provenance study of Albian (uppermost Lower Cretaceous) terrigenous quartz sands and sandstones in southern extra-Carpathian Poland. *Minerals*, **11**, 553.

Kotowski, J., Olszewska-Nejbert, D., Nejbert, K. and Forster, M. 2023. Long-distance transport of clastic material revealed by monazite and muscovite dating: Albian arenites, extra-Carpathian Poland. *Sedimentary Geology*, **446**, 106339.

Kowal-Linka, M., Jastrzębski, M., Krzemińska, E. and Czupyt, Z. 2022. The importance of parameter selection in studies of detrital zircon provenance: An example from Mesozoic deposits of the Bohemian Massif foreland (Poland). *Palaeogeography*, *Palaeoclimatology*, *Palaeoecology*, **599**, 111035.

Krassowska, A. 1976. The Cretaceous between Zamość, Tomaszów Lubelski and Kryłów. *Biuletyn Państwowego Instytutu Geologicznego*, **291**, 51–101. [In Polish with English summary]

Krippner, A., Meinhold, G., Morton, A.C. and von Eynatten, H. 2014. Evaluation of garnet discrimination diagrams using geochemical data of garnets derived from various host rocks. *Sedimentary Geology*, **306**, 36–52.

Kroshko, Y.V. and Koval'chuk, M.S. 2017. Formation and development of the Lower Cretaceous and middle Paleogene river valleys within the central part of the Ukrainian Shield. *Young Scientist*, **6**, 5–9.

Kuhrts, C., Fennel, W. and Seifert, T. 2004. Model studies of transport of sedimentary material in the western Baltic. *Journal of Marine Systems*, **52**, 167–190.

Kutek, J. and Głazek, J. 1972. The Holy Cross area, central Poland, in the Alpine cycle. *Acta Geologica Polonica*, **22**, 603–653.

Lendzion, K. and Wierzbowski, A. 1966. Dokumentacja wynikowa wiercenia Łuków IG-1. Unpublished report, 57 pp. Archives of the Polish Geological Institute; Warszawa.

Leszczyński, K. 1997. The Lower Cretaceous depositional architecture and sedimentary cyclicity in the Mid-Polish Trough. *Geological Quarterly*, **41**, 509–520.

Leszczyński, K. 2010. Lithofacies evolution of the Late Cretaceous basin in the Polish Lowlands. *Biuletyn Państwowego Instytutu Geologicznego,* **443**, 33–54. [In Polish with English summary]

Leszczyński, K. 2012. The internal geometry and lithofacies pattern of the Upper Cretaceous–Danian sequence in the Polish lowlands. *Geological Quarterly*, **56**, 363–386.

Liu, J., Yin, P., Zhang, Y., Song, H., Bi, S., Cao, Z. and Liu, S. 2017. Distribution and provenance of detrital minerals in southern coast of Shandong Peninsula. *Journal of Ocean University of China*, **16**, 747–756.

Machalski, M. and Kennedy, W.J. 2013. Oyster-bioimmured ammonites from the Upper Albian of Annopol, Poland: Stratigraphic and palaeobiogeographic implications. *Acta Geologica Polonica*, **63**, 545–554.

Mannerstrand, M. and Lundqvist, L. 2003. Garnet chemistry from the Slöinge excavation, Halland and additional Swedish and Danish excavations – Comparisons with garnet occurring in a rock context. *Journal of Archaeological Science*, **30**, 169–183.

Małecki, J. 1980. Santonian siliceous sponges from Korzkiew near Kraków (Poland). *Annales Societatis Geologorum Poloniae*, **50**, 409–439.

Mange, M.A. and Morton, A.C. 2007. Geochemistry of heavy minerals. In: Mange, M.A. and Wright, D.T. (Eds), Heavy minerals in use, 345–391. Elsevier B.V.; Amsterdam.

Mange, M.A. and Wright, D.T. 2007. Heavy minerals in use, 1283 pp. Elsevier B.V.; Amsterdam.

Marcinowski, R. 1970. The Cretaceous transgressive deposits east of Częstochowa (Polish Jura Chain). *Acta Geologica Polonica*, **20**, 413–449.

Marcinowski, R. 1974. The transgressive Cretaceous (Upper Albian through Turonian) deposits of the Polish Jura Chain. *Acta Geologica Polonica*, **24**, 117–220.

Marcinowski, R. and Radwański, A. 1983. The Mid-Cretaceous transgression onto the Central Polish Uplands (marginal part of the Central European Basin). *Zitteliana*, **10**, 65–95.

Marcinowski, R. and Radwański, A. 1989. A biostratigraphic approach to the mid-Cretaceous transgressive sequence of the Central Polish Uplands. *Cretaceous Research*, **10**, 153–172.

Marcinowski, R. and Wiedmann, J. 1985. The Albian ammonite fauna of Poland and its palaeogeographical significance. *Acta Geologica Polonica*, **35**, 199–219.

Marcinowski, R. and Wiedmann, J. 1990. The Albian ammonites of Poland. *Palaeontologia Polonica*, **50**, 1–94.

Marek, S. 1988. Palaeothickness, lithofacies and palaeotectonics of the epicontinental Lower Cretaceous in Poland. *Geological Quarterly*, **32**, 157–176. [In Polish with English summary]

Maxbauer, D.P., Feinberg, J.M. and Fox, D.L. 2016. Magnetic mineral assemblages in soils and paleosols as the basis for paleoprecipitation proxies: A review of magnetic methods and challenges. *Earth-Science Reviews*, **155**, 28–48.

Morton, A.C. 1979. Surface features of heavy mineral grains from Palaeocene sands of the central North Sea. *Scottish Journal of Geology*, **15**, 293–300.

Morton, A.C. 1984. Stability of detrital heavy minerals in Tertiary sandstones from the north sea basin. *Clay Minerals*, **19**, 287–308.

Morton, A.C. 1986. Dissolution of apatite in North Sea Jurassic sandstones: implications for the generation of secondary porosity. *Clay Minerals*, **21**, 711–733.

Morton, A.C. 1991. Geochemical studies of detrital heavy minerals and their application to provenance research. *Geological Society Special Publication*, **57**, 31–45.

Morton, A.C. and Hallsworth, C. 2007. Stability of detrital heavy minerals during burial diagenesis. In: Mange, M.A. and Wright, D.T. (Eds), Heavy minerals in use, 215–245. Elsevier B.V.; Amsterdam.

Morton, A.C., Hallsworth, C. and Chalton, B. 2004. Garnet compositions in Scottish and Norwegian basement terrains: A framework for interpretation of North Sea sandstone provenance. *Marine and Petroleum Geology*, **21**, 393–410.

Mücke, A. and Bhadra Chaudhuri, J.N. 1991. The continuous alteration of ilmenite through pseudorutile to leucoxene. *Ore Geology Reviews*, **6**, 25–44.

Mücke, A. and Cabral, A.R. 2005. Redox and nonredox reactions of magnetite and hematite in rocks. *Chemie der Erde*, **65**, 271–278.

Olszewska-Nejbert, D., Kotowski, J. and Nejbert, K. 2020. *Psilonichnus upsilon* Frey, Curran and Pemberton, 1984 burrows and their environmental significance in transgressive Albian (Lower Cretaceous) sands of Glanów-Stroniczki, Cracow Upland, southern Poland. *Palaeogeography*, *Palaeoclimatology*, *Palaeoecology*, **538**, 109388.

Pettijohn, F.J. 1941. Persistence of heavy minerals and geologic age. *The Journal of Geology,* **49**, 610–625.

Pieczka, A., Szuszkiewicz, A., Szełęg, E., Nejbert, K., Łodziński, M., Ilnicki, S., Turniak, K., Banach, M., Hołub, W., Michałowski, P. and Różniak, R. 2013. (Fe,Mn)-(Ti,Sn)-(Nb,Ta) oxide assemblage in a little fractionated portion of a mixed (NYF + LCT) pegmatite from Piława Górna, the Sowie Mts. block, SW Poland. *Journal of Geosciences*, **58**, 91–112.

Pober, E. and Faupl, P. 1988. The chemistry of detrital chromian spinels and its implications for the geodynamic evolution of the Eastern Alps. *Geologische Rundschau*, **77**, 641–670.

Power, M.R., Pirrie, D., Andersen, J.C.O. and Wheeler, P.D. 2000. Testing the validity of chrome spinel chemistry as a provenance and petrogenetic indicator. *Geology*, **28**, 1027–1030.

Ramdohr, P. 1975. Die Erzmineralien und ihre Verwachsungen, 1277 pp. Akademie-Verlag; Berlin.

Rudowski, S. 1962. Microforms of the Baltic shore zone in Poland. *Acta Geologica Polonica*, **12**, 541–579. [In Polish with English summary]

Salata, D. 2013. Heavy minerals as detritus provenance indicators for the Jurassic pre-Callovian palaeokarst infill from the Czatkowice Quarry (Kraków-Wieluń Upland, Poland). *Geological Quarterly*, **57**, 537–550.

Samsonowicz, J. 1925. Esquisse géologique des environs de Rachów sur la Vistule et les transgressions de l'Albien et du Cénomanien dans le sillon nord-européen. *Sprawozdania Polskiego Instytutu Geologicznego*, **3**, 45–118. [In Polish with French summary]

Schönig, J., von Eynatten, H., Tolosana-Delgado, R. and Meinhold, G. 2021. Garnet major-element composition as an indicator of host-rock type: a machine learning approach using the random forest classifier. *Contributions to Mineralogy and Petrology*, **176**, 98.

Schulze, D.J. 2001. Origins of chromian and aluminous spinel macrocrysts from kimberlites in Southern Africa. *Canadian Mineralogist*, **39**, 361–376.

Stephenson, R.A., Narkiewicz, M., Dadlez, R., van Wees, J.-D. and Andriessen, P. 2003. Tectonic subsidence modelling of the Polish Basin in the light of new data on crustal structure and magnitude of inversion. *Sedimentary Geology*, **156**, 59–70.

Szopa, K., Skreczko, S., Chew, D., Krzykawski, T. and Szymczyk, A. 2020. Multi-tool (LA-ICPMS, EMPA and XRD) investigation on heavy minerals from selected Holocene peat-bog deposits from the Upper Vistula river valley, Poland. *Minerals*, **10**, 9.

Świdrowska, J., Hakenberg, M., Poluhtovič, B., Seghedi, A. and Višnâkov, I. 2008. Evolution of the Mesozoic basins on the south western edge of the East European Craton (Poland, Ukraine, Moldova, Romania). *Studia Geologica Polonica*, **130**, 3–130.

Turner, G. and Morton, A.C. 2007. The effects of burial diagenesis on detrital heavy mineral grain surface textures. In: Mange, M.A. and Wright, D.T. (Eds), Heavy minerals in use, 393–412. Elsevier B.V.; Amsterdam.

Velbel, M.A., Mcguire, J.T. and Madden, A.S. 2007. Scanning Electron Microscopy of garnet from southern Michigan soils: etching rates and inheritance of pre-glacial and pre-pedogenic grain-surface textures. In: Mange, M.A. and Wright, D.T. (Eds), Heavy minerals in use, 413–432. Elsevier B.V.; Amsterdam.

Ventura, B. and Lisker, F. 2003. Long-term landscape evolution of the northeastern margin of the Bohemian Massif: apatite fission-track data from the Erzgebirge (Germany). *International Journal of Earth Sciences*, **92**, 691–700.

Wagstaff, B., Gallagh, S.J., Norvick, M.S., Cantrill, D.J. and Wallace, M.W. 2013. High latitude Albian climate vari-

ability: palynological evidence for long-term drying in a greenhouse world. *Palaeogeography*, *Palaeoclimatology*, *Palaeoecology*, **386**, 501–511.

Walaszczyk, I. 1987. Mid-Cretaceous events at the marginal part of the Central European Basin (Annopol-on-Vistula section, Central Poland). *Acta Geologica Polonica*, **37**, 61–74.

Weibel, R. and Friis, H. 2007. Alteration of opaque heavy minerals as a reflection of the geochemical conditions in depositional and diagenetic environments. In: Mange, M.A. and Wright, D.T. (Eds), Heavy minerals in use, 277–303. Elsevier B.V.; Amsterdam.

Ziegler, P. 1988. Evolution of the Arctic-North Atlantic and the Western Tethys: A visual presentation of a series of paleogeographic-paleotectonic maps. *AAPG memoir*, **43**, 164–196.

Ziegler, P. 1990. Geological stlas of Western and Central Europe, 293 pp. Shell Internationale Petroleum Maatschappij, B.V.; Hague.

Żelaźniewicz, A., Aleksandrowski, P., Buła, Z., Karnkowski, P.H., Konon, A., Oszczypko, N., Ślączka, A., Żaba, J. and Żytko, K. 2011. Regionalizacja tektoniczna Polski, 60 pp. Komitet Nauk Geologicznych PAN; Wrocław.

Żelichowski, A. and Rek, E. 1966. Dokumentacja wynikowa otworu oporowego Tomaszów Lubelski IG-1. Unpublished report, 67 pp. Archives of the Polish Geological Institute; Warszawa.

Manuscript submitted: 8th May 2023
Revised version accepted: 3rd December 2023